Supporting Information

Synthesis, photophysical, thermal and antimycobacterial properties of novel 6-amino-2-alkyl(aryl/heteroaryl)-4-(trifluoromethyl) quinolines

Yuri G. Kappenberg, [a] Alex Ketzer, [a] Felipe S. Stefanello, [a] Paulo R. S. Salbego, [a] Thiago V. Acunha,[b] Bruno L. Abbadi, [c] Cristiano V. Bizarro, [c] Luiz A. Basso, [c] Pablo Machado, [c] Marcos A. P. Martins, [a] Nilo Zanatta, [a] Bernardo A. Iglesias [b] and Helio G. Bonacorso*[a]

[a]Núcleo de Química de Heterociclos (NUQUIMHE), Departamento de Química, Universidade Federal de Santa Maria, 97105-900 Santa Maria, Brazil.
E-mail: helio.bonacorso@ufsm.br
[b]Laboratório de Bioinorgânica e Materiais Porfirínicos, Departamento de Química, Universidade Federal de Santa Maria, Santa Maria, RS, 97105-900, Brazil.
[c]Instituto Nacional de Ciência e Tecnologia em Tuberculose (INCT-TB), Centro de Pesquisas em Biologia Molecular e Funcional, Pontifícia Universidade Católica do Rio Grande do Sul, 90619-900 Porto Alegre, RS, Brazil.

1. Synthesis Procedures

Table S1. Optimization of the reaction conditions for compounds **3**.[a]

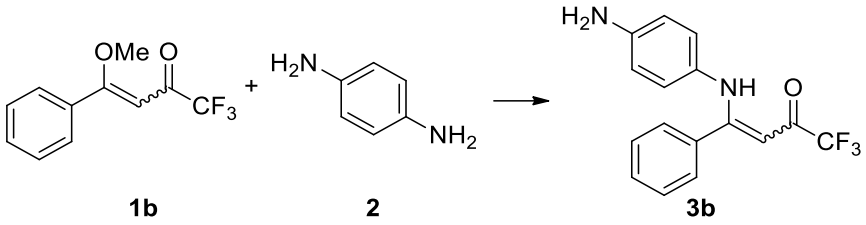

1b **2** **3b**

Entry[a]	Solvent	Temperature (°C)	Yield[b] (%)
1	MeOH	0	87
2	MeOH	25	62
3	EtOH	0	82
4	$CHCl_3$	0	73
5	CH_2Cl_2	0	71
6	CH_3CN	0	71

[a] Reaction conditions: **1b** (1.0 mmol) and **2** (1.0 mmol), solvent (10 mL), 2 h.

[b] Isolated yield.

Synthesis of (*Z*)-4-((4-aminophenyl)amino)-1,1,1-trifluorobut-3-en-2-ones (3a-f)

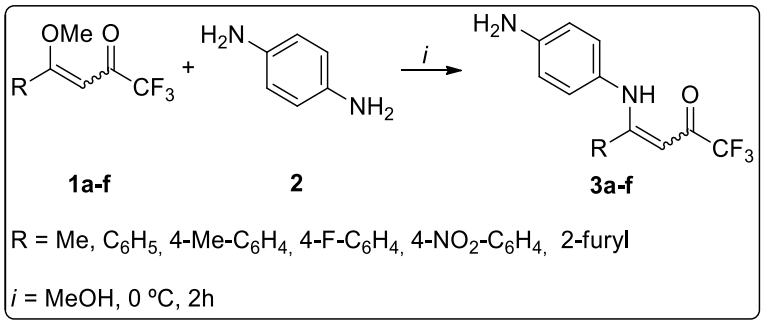

To a magnetically stirred solution of 1,4-phenylenediamine (**2**) (1 mmol, 0.108 g) in methanol (10 mL), a solution of 4-methoxy-1,1,1-trifluorobut-3-en-2-ones (**3a-f**) (1 mmol) in methanol (20mL) was added dropwise at 0 ºC over a period of 2 h. After the end of the reaction, traces of the solvent was evaporated under reduced pressure and the products **3a-f** recrystallized from ethanol and water. The solution was then cooled at -10 °C, and yellow, red or brown solids were obtained. The solids were filtered under reduced pressure, washed with cold water, and dried under reduced pressure.

Synthesis of 2-alkyl(aryl/heteroaryl)-6-amino-4-(trifluormethyl)quinolines

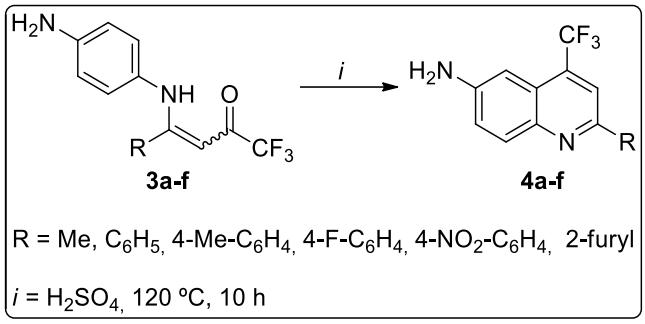

To a flask containing 1 mmol of (*Z*)-4-((4-aminophenyl)amino)-1,1,1-trifluorobut-3-en-2-ones (**3a-f**), 5 mL of the concentrated sulfuric acid was added. The reaction mixture was heated at 120 °C under magnetic stirring for 10 h. After cooling the system to room temperature, the reaction mixture was treated with distilled water (5 mL) and was neutralized with a solution of $NaHCO_3$ saturated. The compounds **4a-f** were extracted with ethyl acetate (3x 20 mL) and the organic phase was dried with Na_2SO_4, filtered, and then the solvent was removed under reduced pressure. The products **4a-f** were purified by column chromatography on silica gel using hexane as eluent.

2. Crystallographic Data

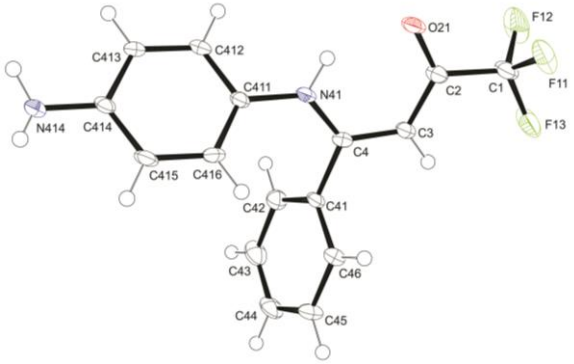

Figure S1. ORTEP of enamino ketone (**3b**) (CCDC 1895628). Displacement ellipsoids are drawn at the 50% probability level.

Table S2. Crystal data and structure refinement for compounds **3b** and **4d**.

Compound	**3b**	**4d**
CCDC number	1895628	1895629
Empirical formula	$C_{16}H_{13}F_3N_2O$	$C_{16}H_{10}F_4N_2$
Molecular weight	306.28	306.26
Temperature (K)	100(2)	296(2)
Wavelength (Å)	0.71073	1.54178
Crystal system	Monoclinic	Monoclinic
Space group	$P2_1/c$	$P2_1/c$
Cell parameters		
a (Å)	12.0703(9)	14.122(3)
b (Å)	5.8282(4)	4.6032(10)
c (Å)	20.5755(14)	21.574(5)
α (°)	90	90
β (°)	100.792(2)	106.541(11)
γ (°)	90	90
Volume ($Å^3$)	1421.85(17)	1344.4(5)
Z	4	4
Calculated density (Mg/m^3)	1.431	1.513
Abs. coef. (mm^{-1})	0.118	1.126
F (000)	632	624
Crystal size (mm)	0.397 x 0.091 x 0.055	0.318 x 0.248 x 0.094
θ range for data collection (°)	2.391 to 27.152	3.264 to 68.481
h, k, l range	-15<=h<=15, -7<=k<=7, -26<=l<=26	-16<=h<=16, -5<=k<=4, -26<=l<=25
Reflections collected / unique	38690 / 3156 [R(int) = 0.0919]	8521 / 2353 [R(int) = 0.0199]
Completeness to theta (%)	99.8	91.4
Absorption correction	Multi-scan	Multi-scan
Max. and min. transmission	0.7455 and 0.5601	0.7531 and 0.6708
Refinement method	Full-matrix least-squares on F^2	Full-matrix least-squares on F^2
Data / restraints / parameters	3156 / 3 / 204	2353 / 2 / 200
Goodness-of-fit on F^2	1.056	1.019
Final R indices	R1 = 0.0585, wR2 = 0.1377	R1 = 0.0359, wR2 = 0.0931
R all data	R1 = 0.0830, wR2 = 0.1505	R1 = 0.0485, wR2 = 0.1026
Extinction coefficient	none	none
$\Delta\rho_{max.}$ and $\Delta\rho_{min}$ ($e\ A^{-3}$)	0.572 and -0.457	0.134 and -0.130

3. UV-Vis Analyses

UV-Vis absorption spectra were recorded using Shimadzu UV-2600 spectrophotometer (data interval, 1.0 nm) using $CHCl_3$, DMSO or MeOH as solvent, using concentration of 2.0 x 10^{-4} M for each compound. Fluorescence spectra of samples in all solutions were measured with a Varian Cary50 fluorescence spectrophotometer (emission; slit 1.0 mm) and were corrected according to the manufacturer's instructions. The lowest energy electronic transition of each derivative to be excited (emission spectrum) was chosen. Fluorescence quantum yields (Φ_f) of the related compounds in solutions were determined by comparing the corrected fluorescence spectra with that of 9,10-diphenylanthracene (DPA) in chloroform Φ_f = 0.65, λ_{ex} = 366 nm) as the standard as the fluorescence yield.

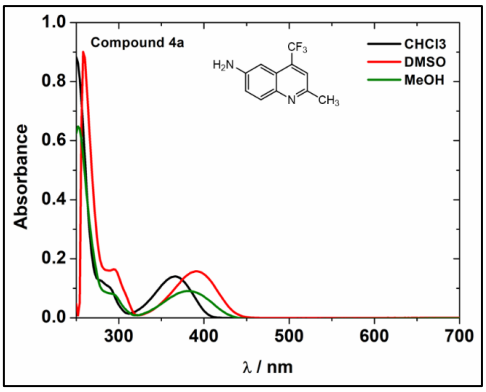

Figure S2. UV-vis spectra of compound **4a** in $CHCl_3$ (black line), DMSO (red line) and MeOH (green line) solution, respectively.

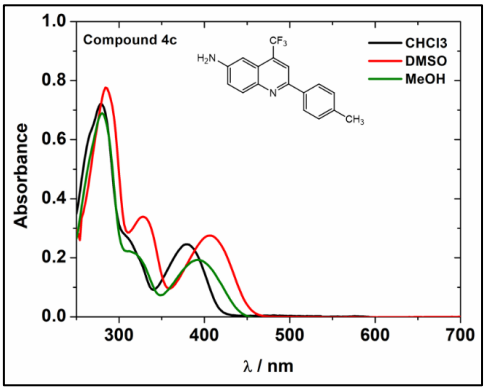

Figure S3. UV-vis spectra of compound **4c** in $CHCl_3$ (black line), DMSO (red line) and MeOH (green line) solution, respectively.

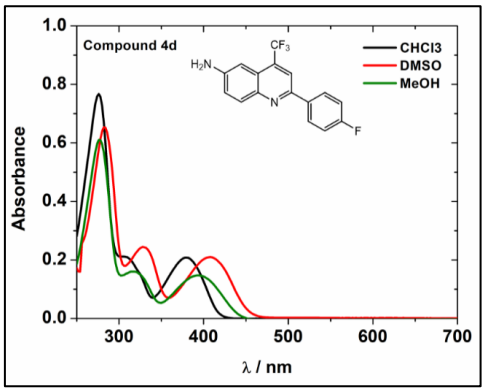

Figure S4. UV-vis spectra of compound **4d** in $CHCl_3$ (black line), DMSO (red line) and MeOH (green line) solution, respectively.

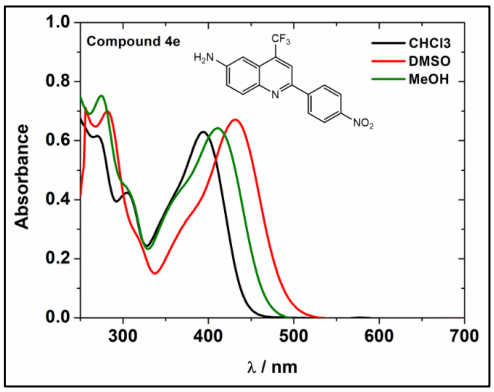

Figure S5. UV-vis spectra of compound **4e** in $CHCl_3$ (black line), DMSO (red line) and MeOH (green line) solution, respectively.

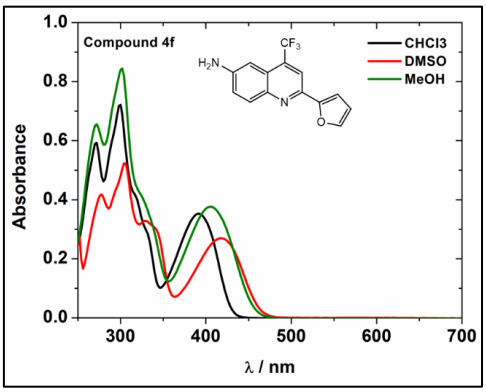

Figure S6. UV-Vis spectra of compound **4f** in $CHCl_3$ (black line), DMSO (red line) and MeOH (green line) solution, respectively.

4. Steady-state emission fluorescence analyses

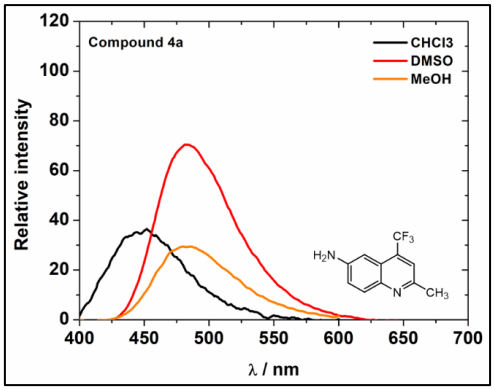

Figure S7. Steady-state emission fluorescence spectra of compound **4a** in $CHCl_3$ (black line; λ_{exc} = 366 nm), DMSO (red line; λ_{exc} = 391 nm) and MeOH (orange line; λ_{exc} = 382 nm) solution, respectively.

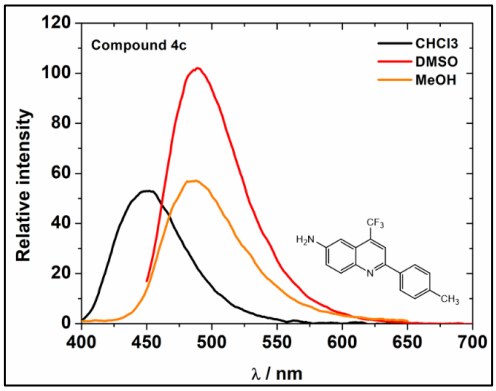

Figure S8. Steady-state emission fluorescence spectra of compound **4c** in $CHCl_3$ (black line; λ_{exc} = 380 nm), DMSO (red line; λ_{exc} = 407 nm) and MeOH (orange line; λ_{exc} = 394 nm) solution, respectively.

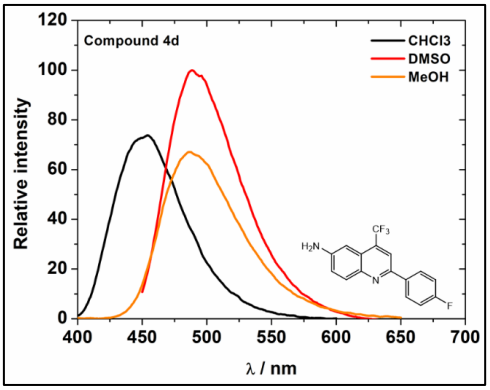

Figure S9. Steady-state emission fluorescence spectra of compound **4d** in $CHCl_3$ (black line; λ_{exc} = 380 nm), DMSO (red line; λ_{exc} = 408 nm) and MeOH (orange line; λ_{exc} = 394 nm) solution, respectively.

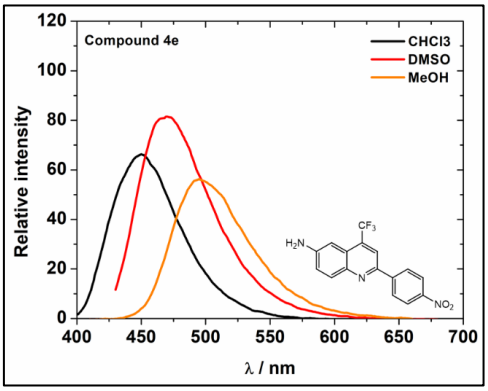

Figure S10. Steady-state emission fluorescence spectra of compound **4e** in $CHCl_3$ (black line; λ_{exc} = 349 nm), DMSO (red line; λ_{exc} = 431 nm) and MeOH (orange line; λ_{exc} = 411 nm) solution, respectively.

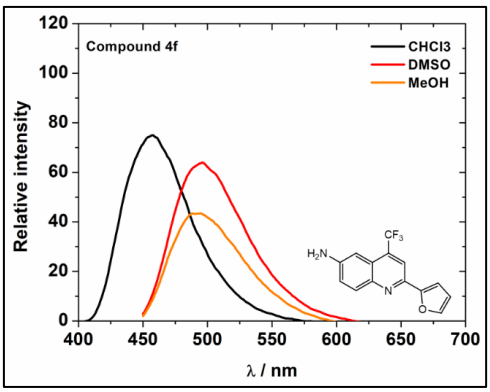

Figure S11. Steady-state emission fluorescence spectra of compound **4f** in $CHCl_3$ (black line; λ_{exc} = 392 nm), DMSO (red line; λ_{exc} = 418 nm) and MeOH (orange line; λ_{exc} = 405 nm) solution, respectively.

5. TD-DFT Calculations

Table S3. Excitation energy (E), wavelength of maximum absorbance (λ_{max}), and oscillator strengths (*f*) for HOMO-LUMO orbitals in $CHCl_3$, DMSO and MeOH for compound **4a**. Calculated at the TD-DFT (SCRF(PCM))-B3LYP/cc-pVTZ level.

Solvent	Electronic Transitions	Energy (eV)	λ_{max} (nm)	Main Orbital Transition	*f*
	$S_0 \rightarrow S_1$	3.429	361.54	HOMO → LUMO (0.69)	0.1284
$CHCl_3$	$S_0 \rightarrow S_2$	4.254	291.49	HOMO-2 → LUMO (0.70)	0.0012
	$S_0 \rightarrow S_3$	4.336	285.92	HOMO-1 → LUMO (0.53)	0.0007
	$S_0 \rightarrow S_1$	3.404	364.21	HOMO → LUMO (0.69)	0.1273
DMSO	$S_0 \rightarrow S_2$	4.290	289.02	HOMO-2 → LUMO (0.70)	0.0012
	$S_0 \rightarrow S_3$	4.327	286.54	HOMO-1 → LUMO (0.52)	0.0009
	$S_0 \rightarrow S_1$	3.411	363.46	HOMO → LUMO (0.69)	0.1207
MeOH	$S_0 \rightarrow S_2$	4.288	289.12	HOMO-2 → LUMO (0.70)	0.0012
	$S_0 \rightarrow S_3$	4.329	286.41	HOMO-1 → LUMO (0.52)	0.0009

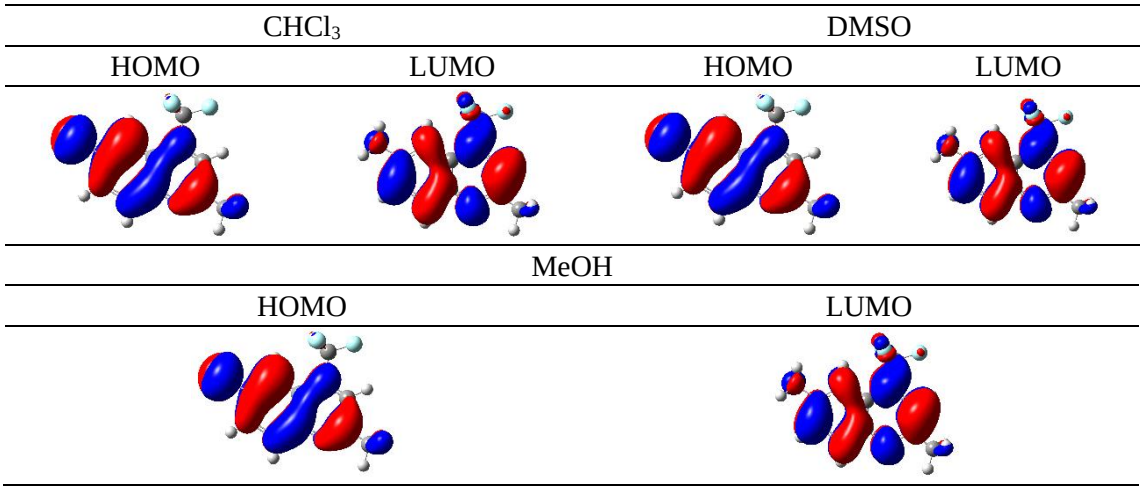

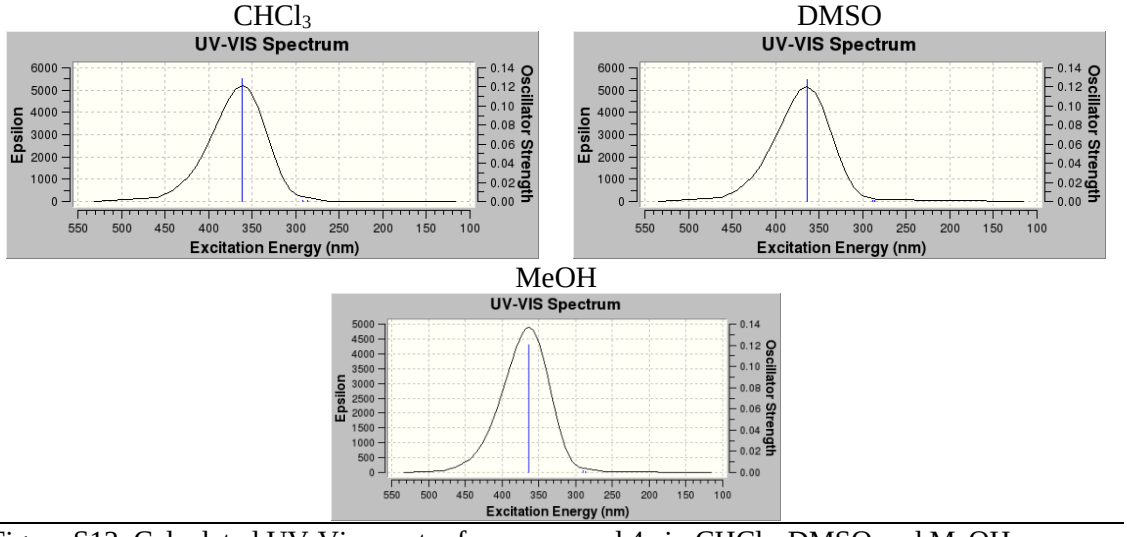

Figure S12. Calculated UV-Vis spectra for compound 4a in $CHCl_3$, DMSO and MeOH.

Table S4. Excitation energy (E), wavelength of maximum absorbance (λ_{max}), and oscillator strengths (*f*) for HOMO-LUMO orbitals in $CHCl_3$, DMSO and MeOH for compound **4b**. Calculated at the TD-DFT (SCRF(PCM))-B3LYP/cc-pVTZ level.

Solvent	Electronic Transitions	Energy (eV)	λ_{max} (nm)	Main Orbital Transition	*f*
	$S_0 \rightarrow S_1$	3.238	382.93	HOMO -> LUMO (0.69)	0.2805
$CHCl_3$	$S_0 \rightarrow S_2$	3.952	313.76	HOMO -> LUMO+1 (0.59)	0.1643
	$S_0 \rightarrow S_3$	4.115	301.32	HOMO-4 -> LUMO (0.63)	0.0016
	$S_0 \rightarrow S_1$	3.213	385.92	HOMO -> LUMO (0.69)	0.2761
DMSO	$S_0 \rightarrow S_2$	3.938	314.82	HOMO -> LUMO+1 (0.60)	0.1606
	$S_0 \rightarrow S_3$	4.147	298.96	HOMO-4 -> LUMO (0.63)	0.0024
	$S_0 \rightarrow S_1$	3.222	384.78	HOMO -> LUMO (0.69)	0.2613
MeOH	$S_0 \rightarrow S_2$	3.942	314.50	HOMO -> LUMO+1 (0.59)	0.1485
	$S_0 \rightarrow S_3$	4.146	299.05	HOMO-4 -> LUMO (0.63)	0.0022

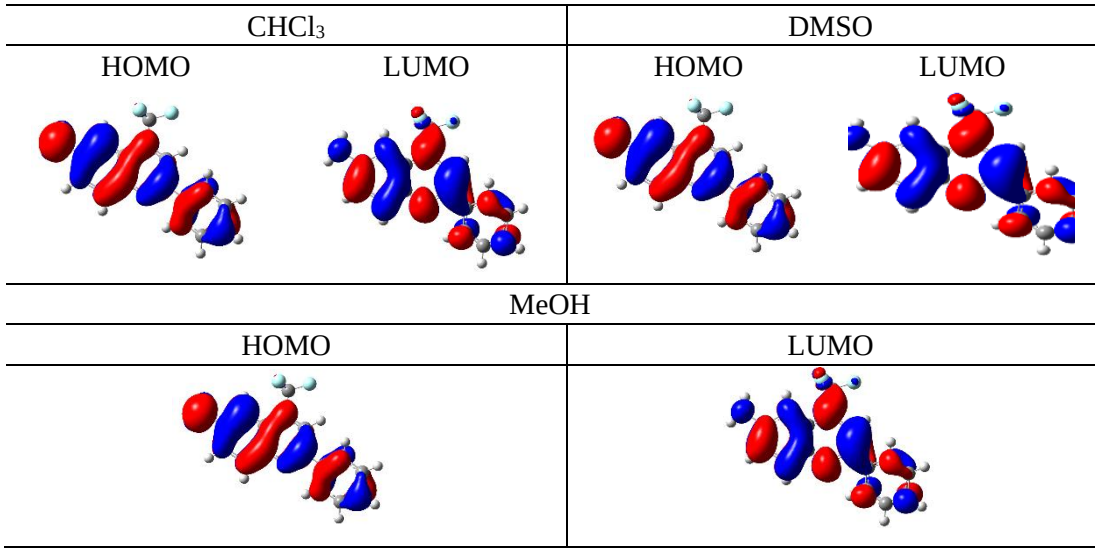

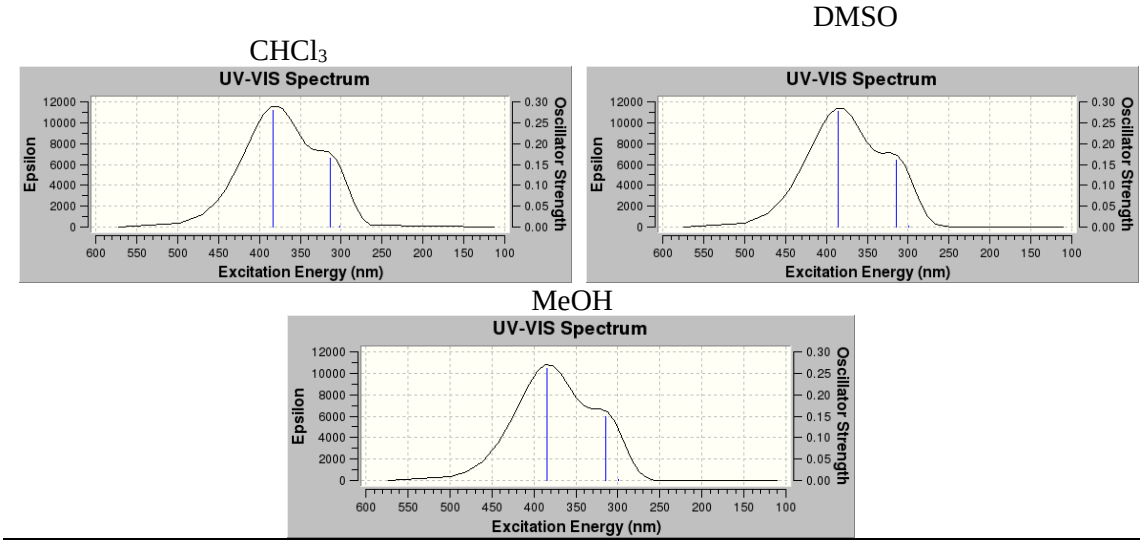

Figure S13. Calculated UV-Vis spectra for compound **4b** in $CHCl_3$, DMSO and MeOH.

Table S5. Excitation energy (E), wavelength of maximum absorbance (λ_{max}), and oscillator strengths (*f*) for HOMO-LUMO orbitals in $CHCl_3$, DMSO and MeOH for compound **4c**. Calculated at the TD-DFT (SCRF(PCM))-B3LYP/cc-pVTZ level.

Solvent	Electronic Transitions	Energy (eV)	λ_{max} (nm)	Main Orbital Transition	*f*
	$S_0 \rightarrow S_1$	3.215	385.65	HOMO → LUMO (0.69)	0.3028
$CHCl_3$	$S_0 \rightarrow S_2$	3.941	314.62	HOMO → LUMO+1 (0.59)	0.1902
	$S_0 \rightarrow S_3$	4.114	301.35	HOMO-4 → LUMO (0.63)	0.0071
	$S_0 \rightarrow S_1$	3.191	388.53	HOMO → LUMO (0.69)	0.2977
DMSO	$S_0 \rightarrow S_2$	3.930	315.48	HOMO → LUMO+1 (0.59)	0.1819
	$S_0 \rightarrow S_3$	4.145	299.12	HOMO-4 → LUMO (0.61)	0.0270
	$S_0 \rightarrow S_1$	3.201	387.39	HOMO → LUMO (0.69)	0.2822
MeOH	$S_0 \rightarrow S_2$	3.934	315.17	HOMO → LUMO+1 (0.58)	0.1674
	$S_0 \rightarrow S_3$	4.144	299.18	HOMO-4 → LUMO (0.62)	0.0200

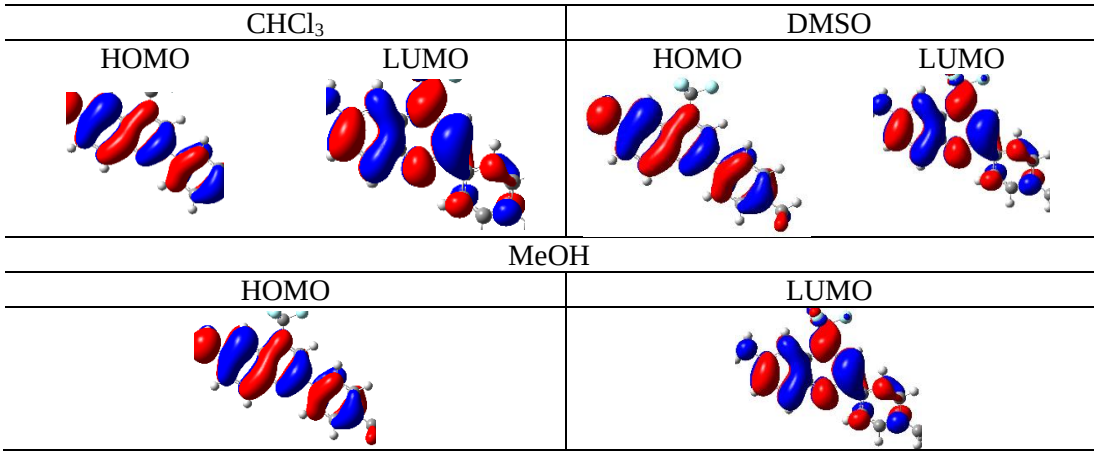

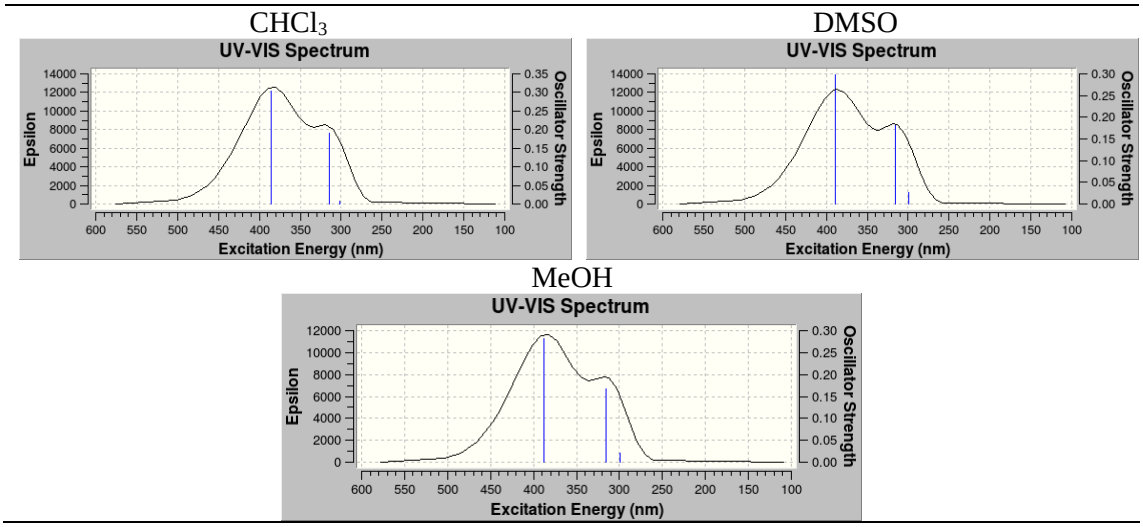

Figure S14. Calculated UV-Vis spectra for compound **4c** in $CHCl_3$, DMSO and MeOH.

Table S6. Excitation energy (E), wavelength of maximum absorbance (λ_{max}), and oscillator strengths (*f*) for HOMO-LUMO orbitals in $CHCl_3$, DMSO and MeOH for compound **4d**. Calculated at the TD-DFT (SCRF(PCM))-B3LYP/cc-pVTZ level.

Solvent	Electronic Transitions	Energy (eV)	λ_{max} (nm)	Main Orbital Transition	*f*
	$S_0 \rightarrow S_1$	3.22	385.23	HOMO → LUMO (0.69)	0.2717
$CHCl_3$	$S_0 \rightarrow S_2$	3.95	313.84	HOMO → LUMO+1 (0.59)	0.1608
	$S_0 \rightarrow S_3$	4.14	299.67	HOMO-3 → LUMO (0.52)	0.0035
	$S_0 \rightarrow S_1$	3.198	387.70	HOMO → LUMO (0.69)	0.2682
DMSO	$S_0 \rightarrow S_2$	3.941	314.62	HOMO → LUMO+1 (0.59)	0.1554
	$S_0 \rightarrow S_3$	4.167	297.54	HOMO-3 → LUMO (0.48)	0.0070
	$S_0 \rightarrow S_1$	3.207	386.61	HOMO → LUMO (0.69)	0.2540
MeOH	$S_0 \rightarrow S_2$	3.944	314.34	HOMO → LUMO+1 (0.58)	0.1436
	$S_0 \rightarrow S_3$	4.166	297.61	HOMO-3 → LUMO (0.49)	0.0058

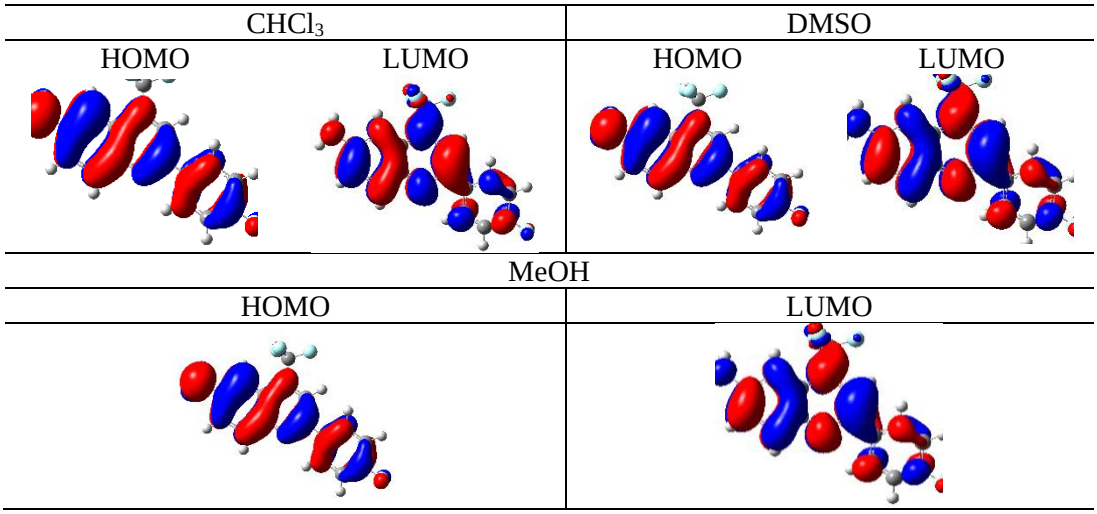

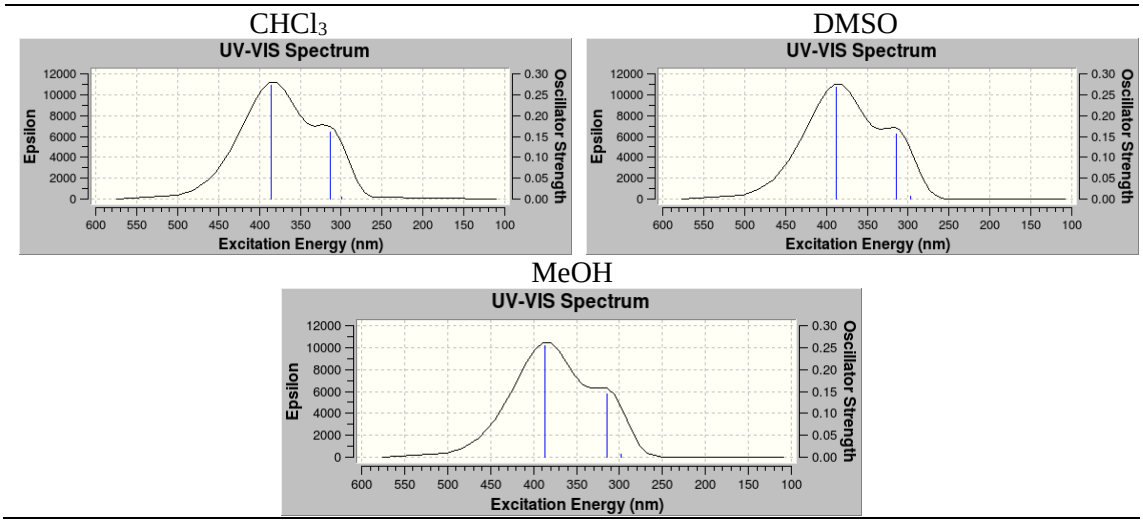

Figure S15. Calculated UV-Vis spectra for compound **4d** in $CHCl_3$, DMSO and MeOH.

Table S7. Excitation energy (E), wavelength of maximum absorbance (λ_{max}), and oscillator strengths (*f*) for HOMO-LUMO orbitals in $CHCl_3$, DMSO and MeOH for compound **4e**. Calculated at the TD-DFT (SCRF(PCM))-B3LYP/cc-pVTZ level.

Solvent	Electronic Transitions	Energy (eV)	λ_{max} (nm)	Main Orbital Transition	*f*
	$S_0 \rightarrow S_1$	2.746	451.57	HOMO → LUMO (0.70)	0.5278
$CHCl_3$	$S_0 \rightarrow S_2$	3.351	370.03	HOMO → LUMO+1 (0.69)	0.0640
	$S_0 \rightarrow S_3$	3.782	327.83	HOMO-1 → LUMO (0.66)	0.1102
	$S_0 \rightarrow S_1$	2.647	468.34	HOMO → LUMO (0.70)	0.5059
DMSO	$S_0 \rightarrow S_2$	3.313	374.19	HOMO → LUMO+1 (0.69)	0.0746
	$S_0 \rightarrow S_3$	3.708	334.38	HOMO-1 → LUMO (0.68)	0.1024
	$S_0 \rightarrow S_1$	2.662	465.74	HOMO → LUMO (0.70)	0.4867
MeOH	$S_0 \rightarrow S_2$	3.319	373.51	HOMO → LUMO+1 (0.69)	0.0712
	$S_0 \rightarrow S_3$	3.714	333.82	HOMO-1 → LUMO (0.68)	0.0982

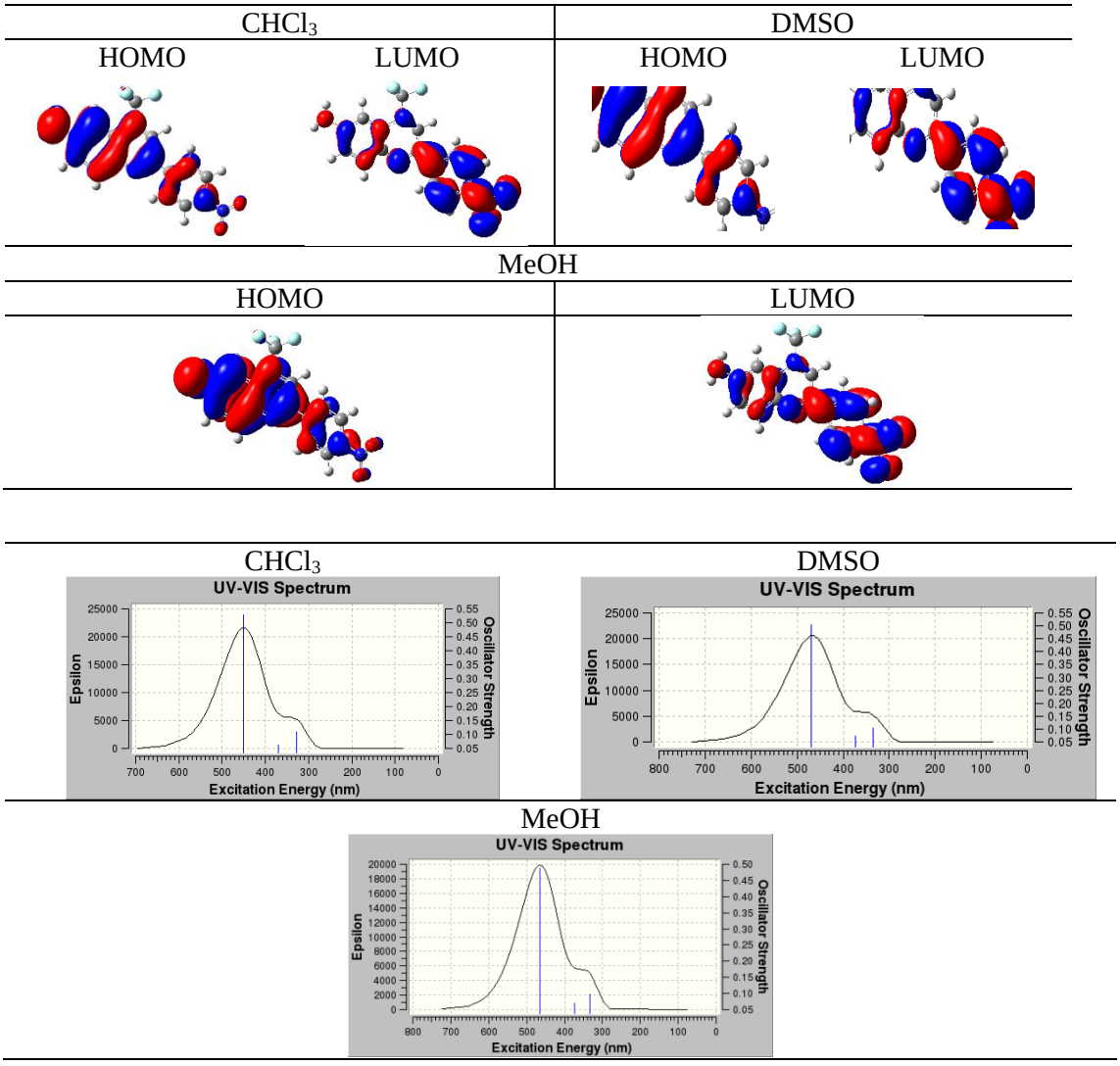

Figure S16. Calculated UV-Vis spectra for compound **4e** in $CHCl_3$, DMSO and MeOH.

Table S8. Excitation energy (E), wavelength of maximum absorbance (λ_{max}), and oscillator strengths (*f*) for HOMO-LUMO orbitals in $CHCl_3$, DMSO and MeOH for compound **4f**. Calculated at the TD-DFT (SCRF(PCM))-B3LYP/cc-pVTZ level.

Solvent	Electronic Transitions	Energy (eV)	λ_{max} (nm)	Main Orbital Transition	*f*
	$S_0 \rightarrow S_1$	3.138	395.08	HOMO → LUMO (0.69)	0.3412
$CHCl_3$	$S_0 \rightarrow S_2$	3.842	322.67	HOMO → LUMO+1 (0.58)	0.2074
	$S_0 \rightarrow S_3$	4.118	301.05	HOMO-1 → LUMO (0.61)	0.5563
	$S_0 \rightarrow S_1$	3.115	398.08	HOMO → LUMO (0.69)	0.3390
DMSO	$S_0 \rightarrow S_2$	3.828	323.93	HOMO → LUMO+1 (0.58)	0.1906
	$S_0 \rightarrow S_3$	4.106	301.95	HOMO-1 → LUMO (0.61)	0.5685
	$S_0 \rightarrow S_1$	3.126	396.65	HOMO → LUMO (0.69)	0.3195
MeOH	$S_0 \rightarrow S_2$	3.832	323.52	HOMO → LUMO+1 (0.57)	0.1748
	$S_0 \rightarrow S_3$	4.119	301.02	HOMO-1 → LUMO (0.60)	0.5600

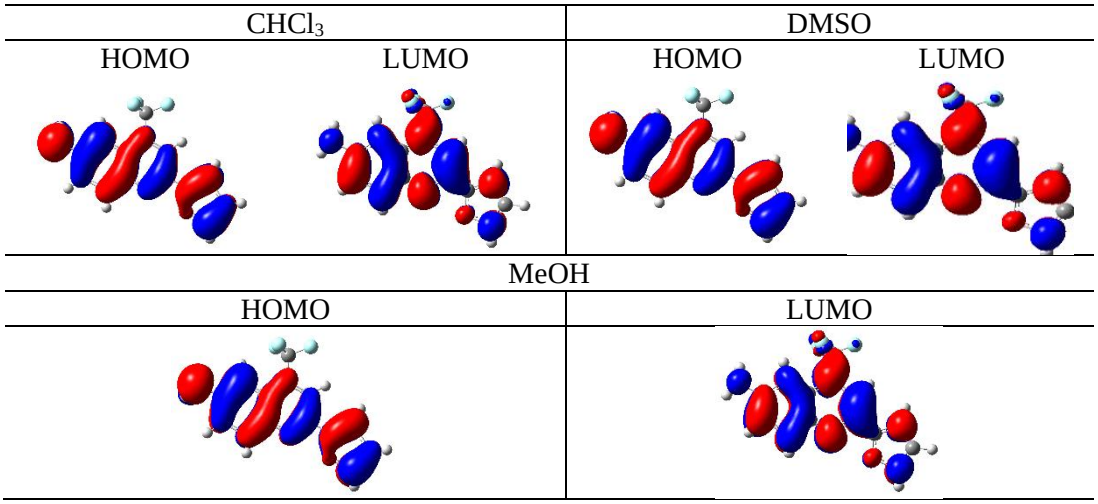

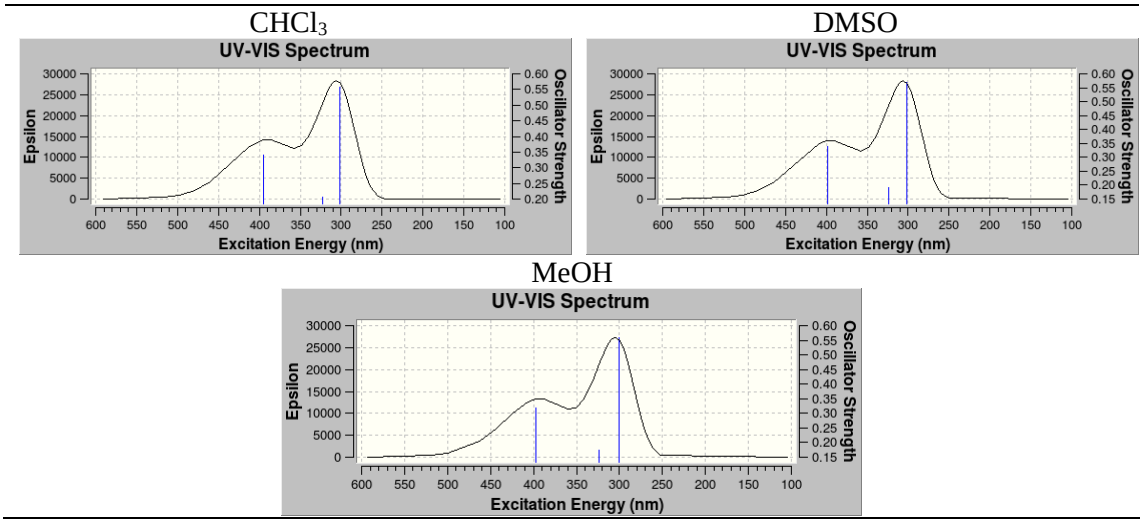

Figure S17. Calculated UV-Vis spectra for compound **4f** in $CHCl_3$, DMSO and MeOH.

6. Thermal Analyses

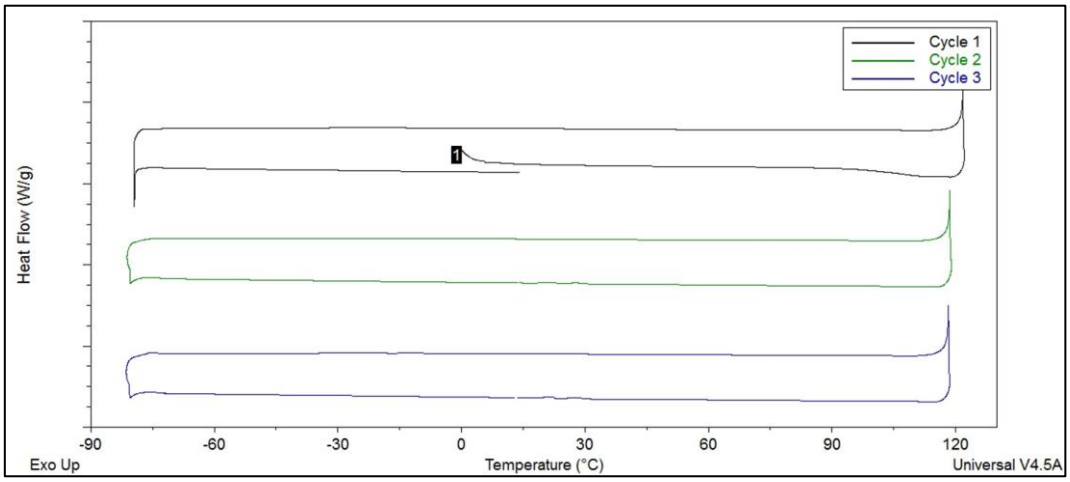

Figure S18. DSC curves for compound **4a** showing the three heating-cooling cycles.

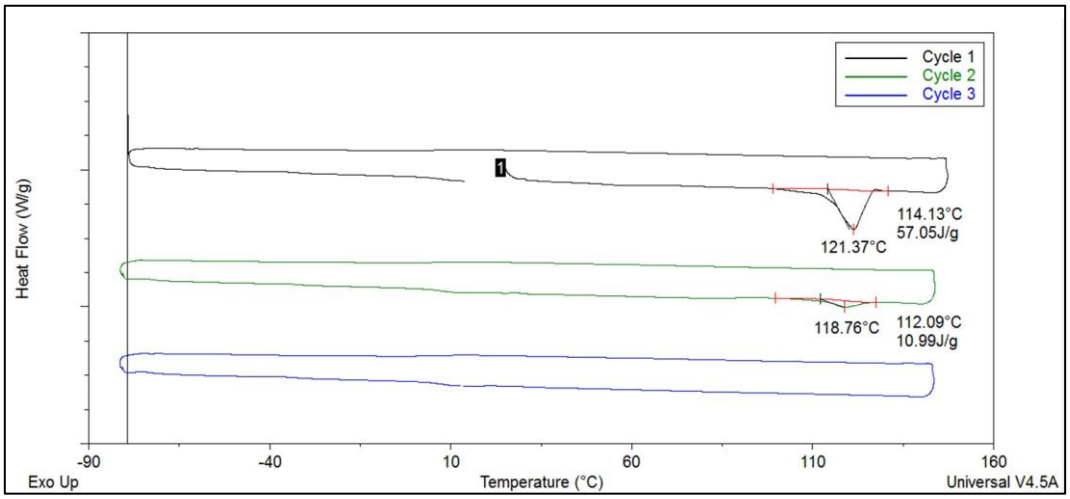

Figure S19. DSC curves for compound **4b** showing the three heating-cooling cycles.

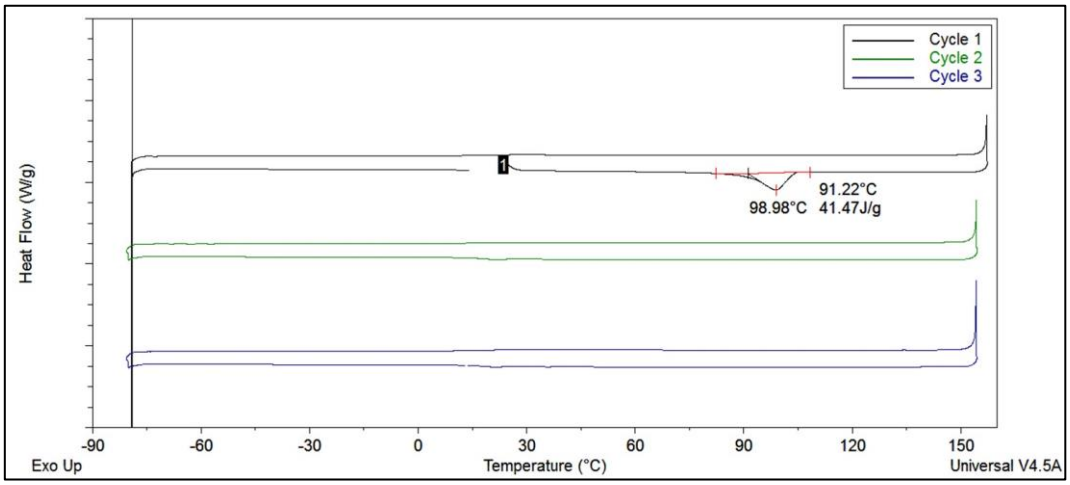

Figure S20. DSC curves for compound **4c** showing the three heating-cooling cycles.

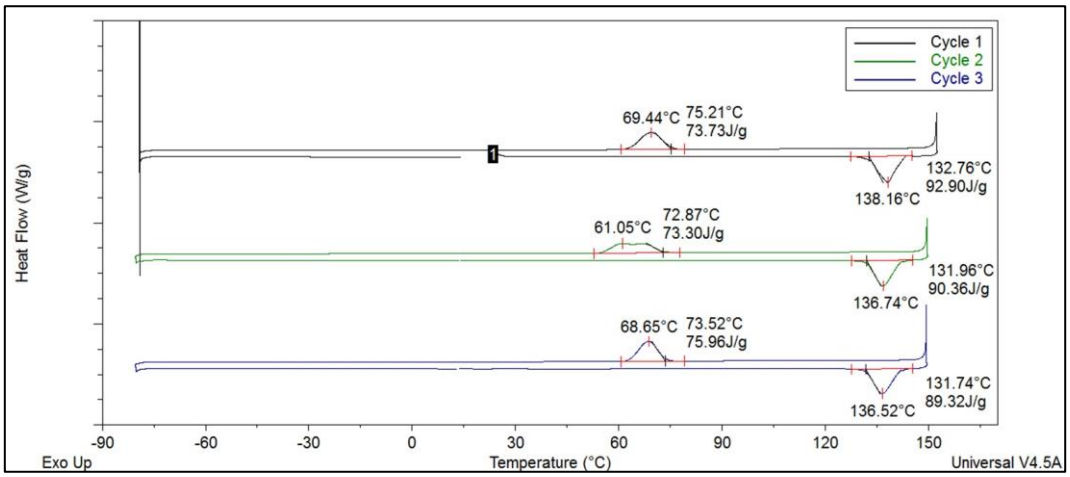

Figure S21. DSC curves for compound **4d** showing the three heating-cooling cycles.

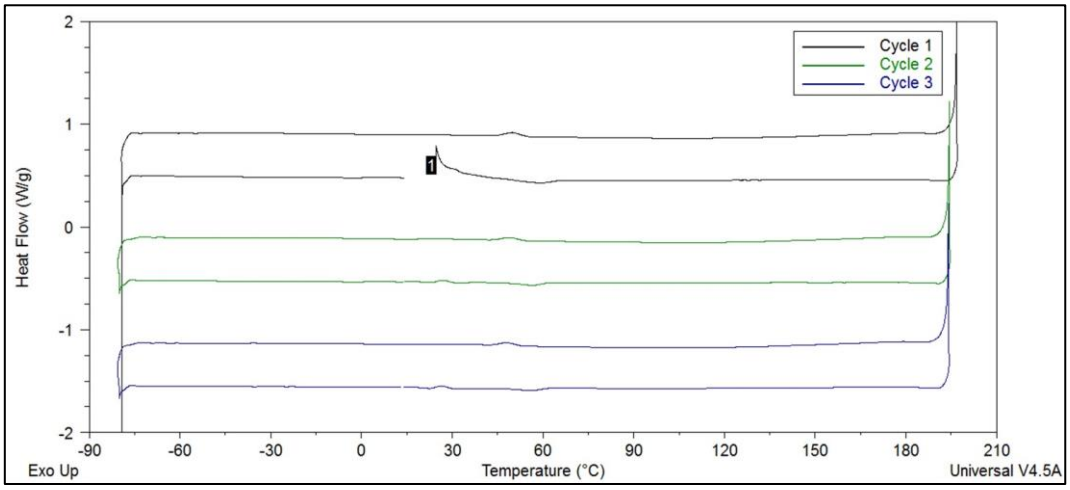

Figure S22. DSC curves for compound **4e** showing the three heating-cooling cycles.

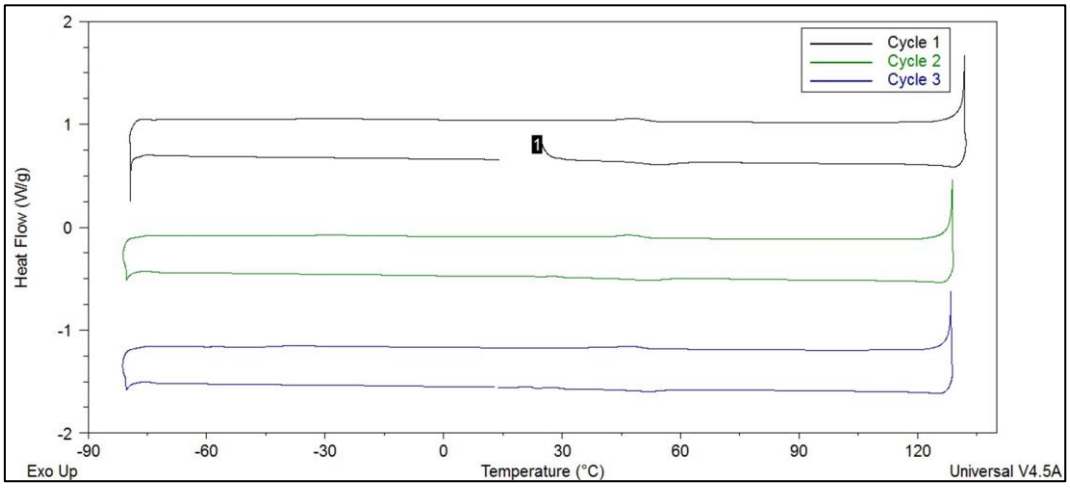

Figure S23. DSC curves for compound **4f** showing the three heating-cooling cycles.

7. ^{1}H, ^{13}C and ^{19}F NMR Spectra

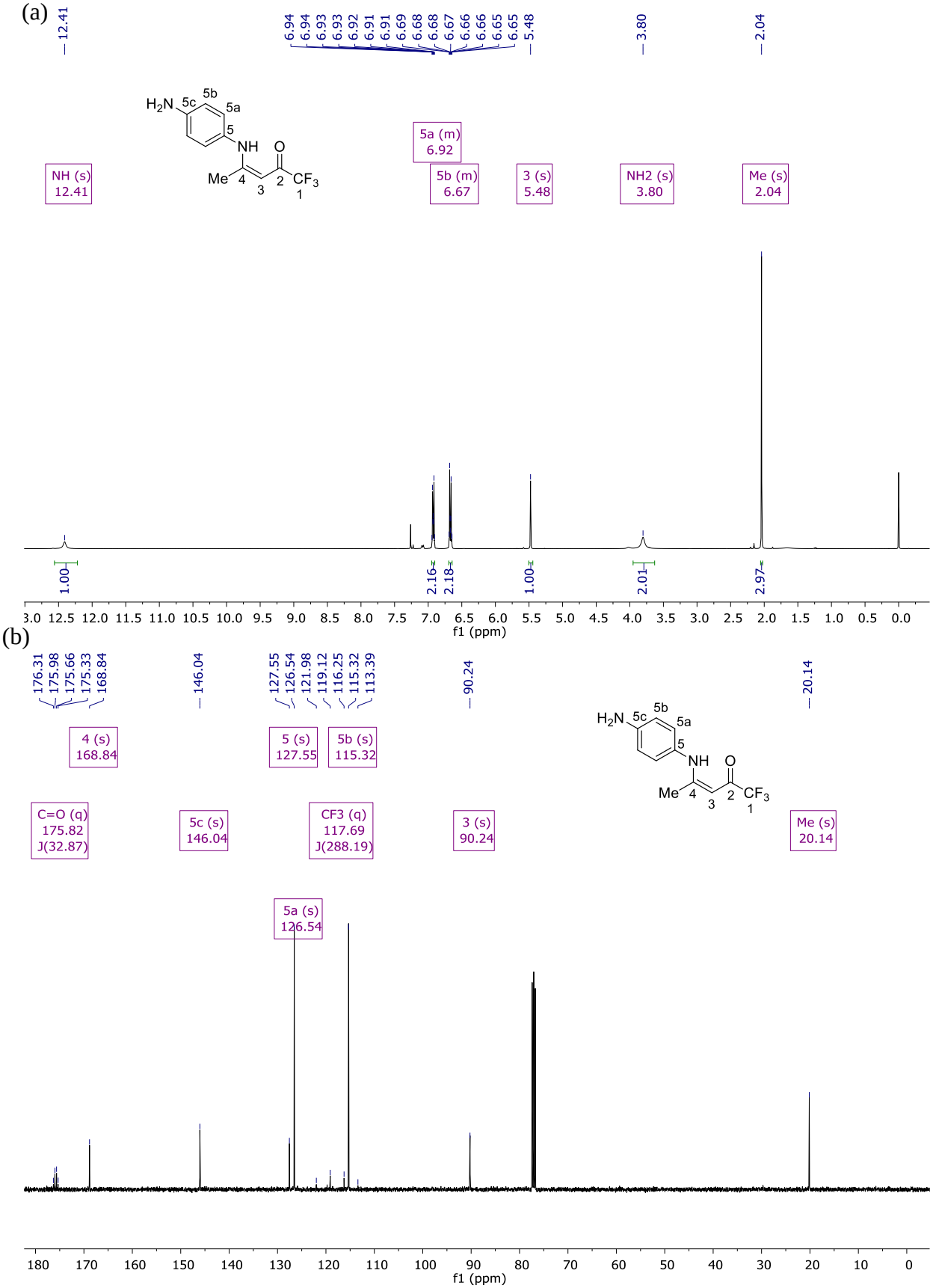

Figure S24. (a) ^{1}H (400 MHz) and (b) ^{13}C (100 MHz) NMR spectra of **3a** in $CDCl_3$.

Figure S25. (a) ^{1}H (400 MHz) and (b) ^{13}C (100 MHz) NMR spectra of **3b** in $CDCl_3$.

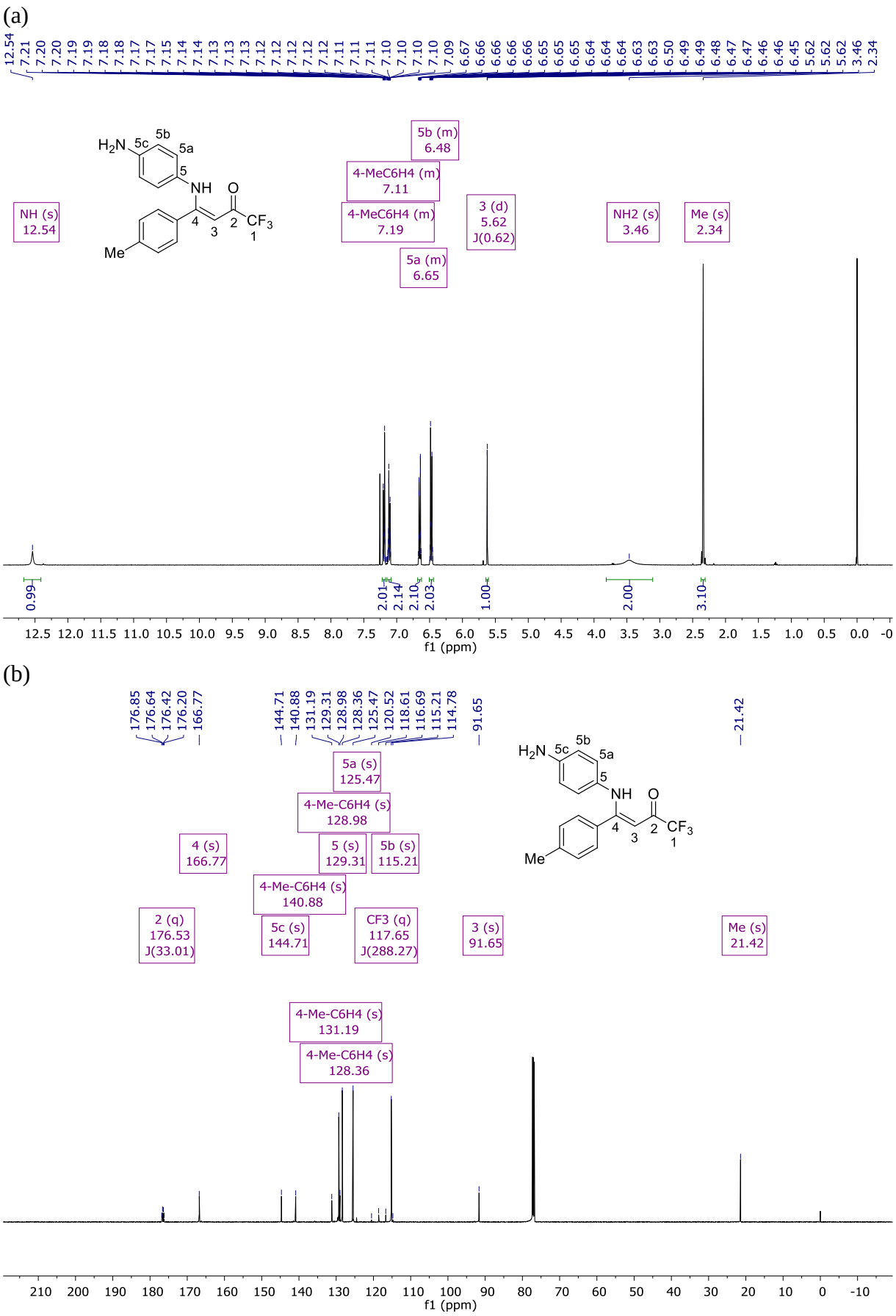

Figure S26. (a) ^{1}H (400 MHz) and (b) ^{13}C (150 MHz) NMR spectra of **3c** in $CDCl_3$.

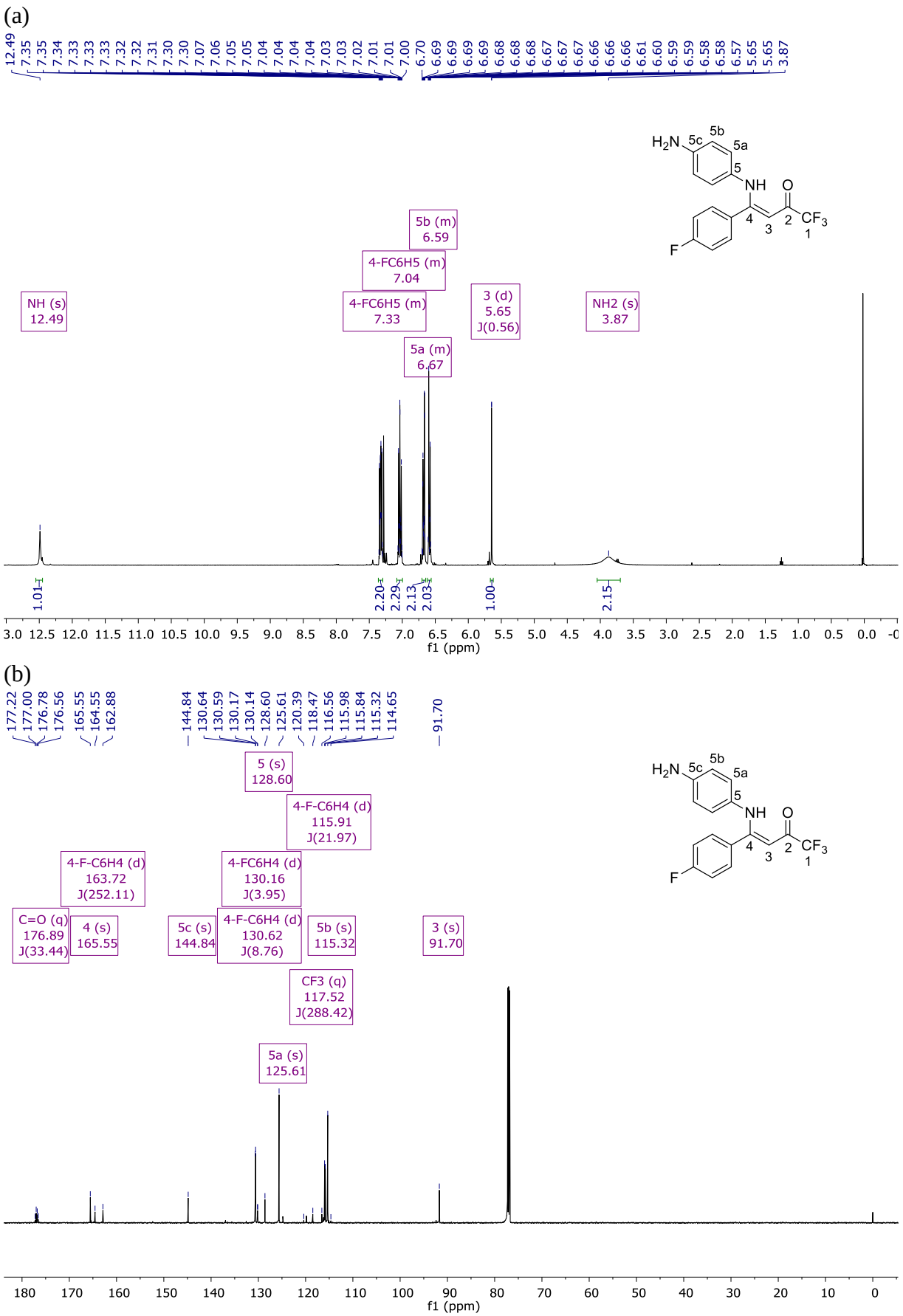

Figure S27. (a) ^{1}H (400 MHz) and (b) ^{13}C (150 MHz) NMR spectra of **3d** in $CDCl_3$.

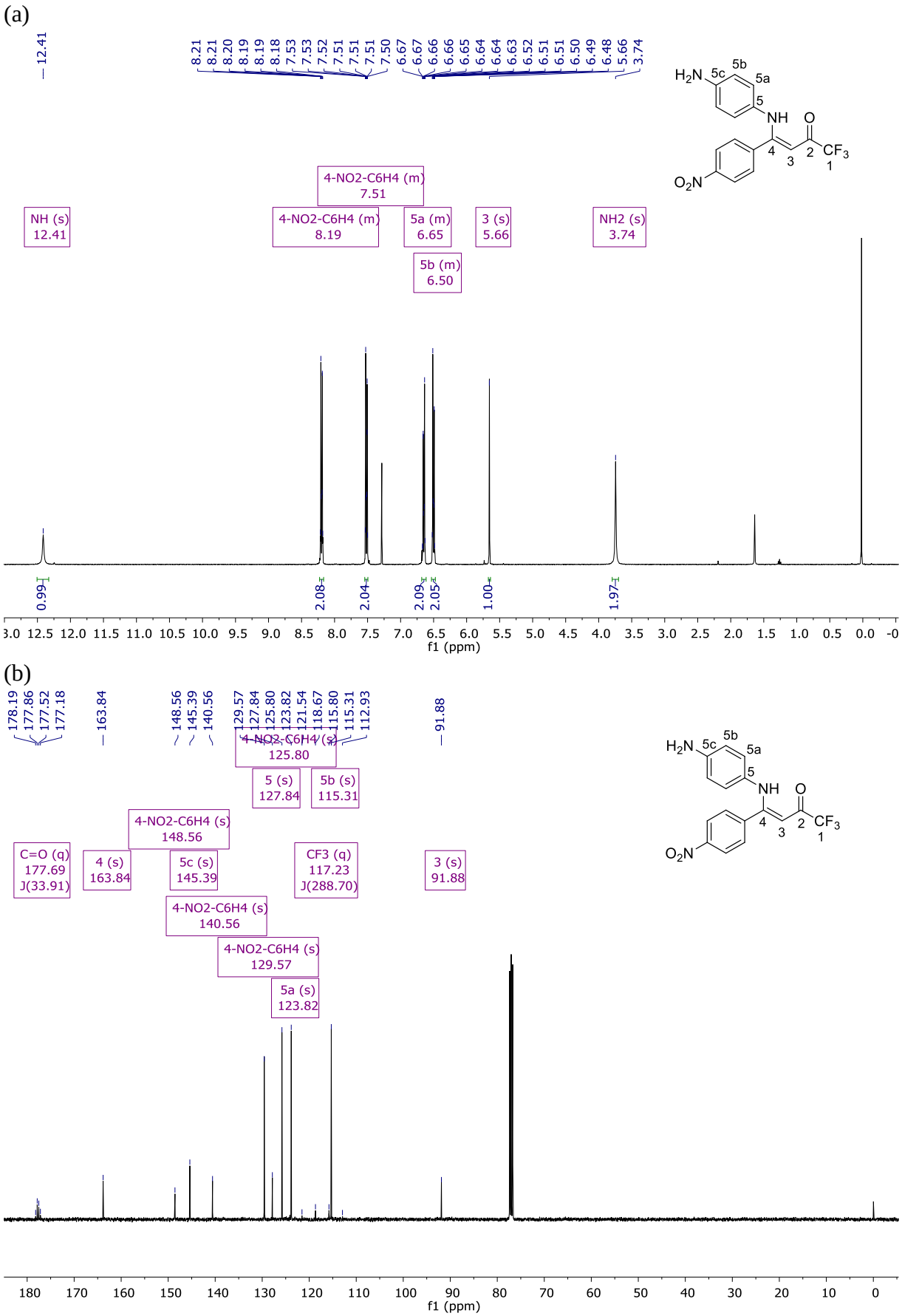

Figure S28. (a) ^{1}H (400 MHz) and (b) ^{13}C (100 MHz) NMR spectra of **3e** in $CDCl_3$.

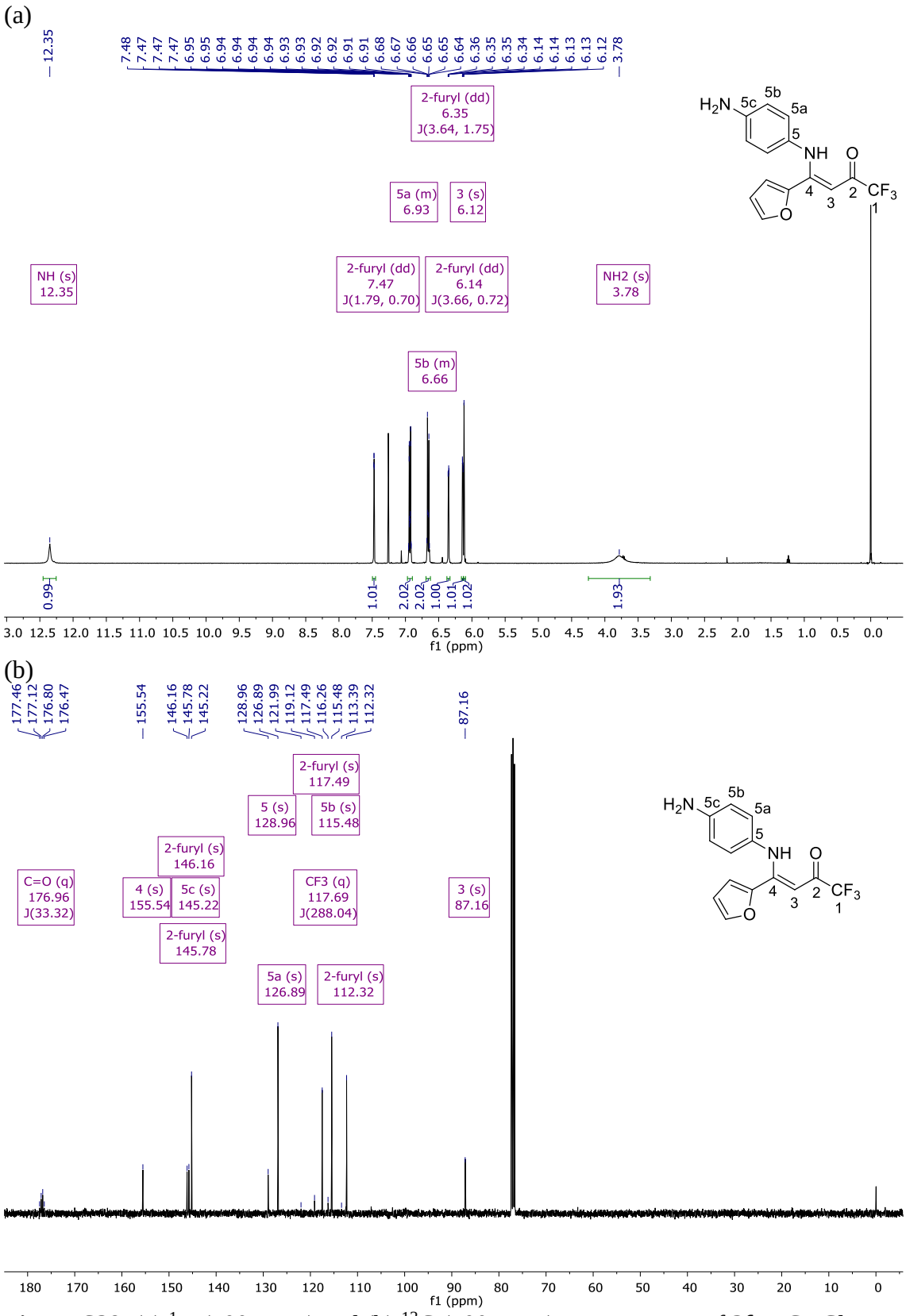

Figure S29. (a) ^{1}H (400 MHz) and (b) ^{13}C (100 MHz) NMR spectra of **3f** in $CDCl_3$.

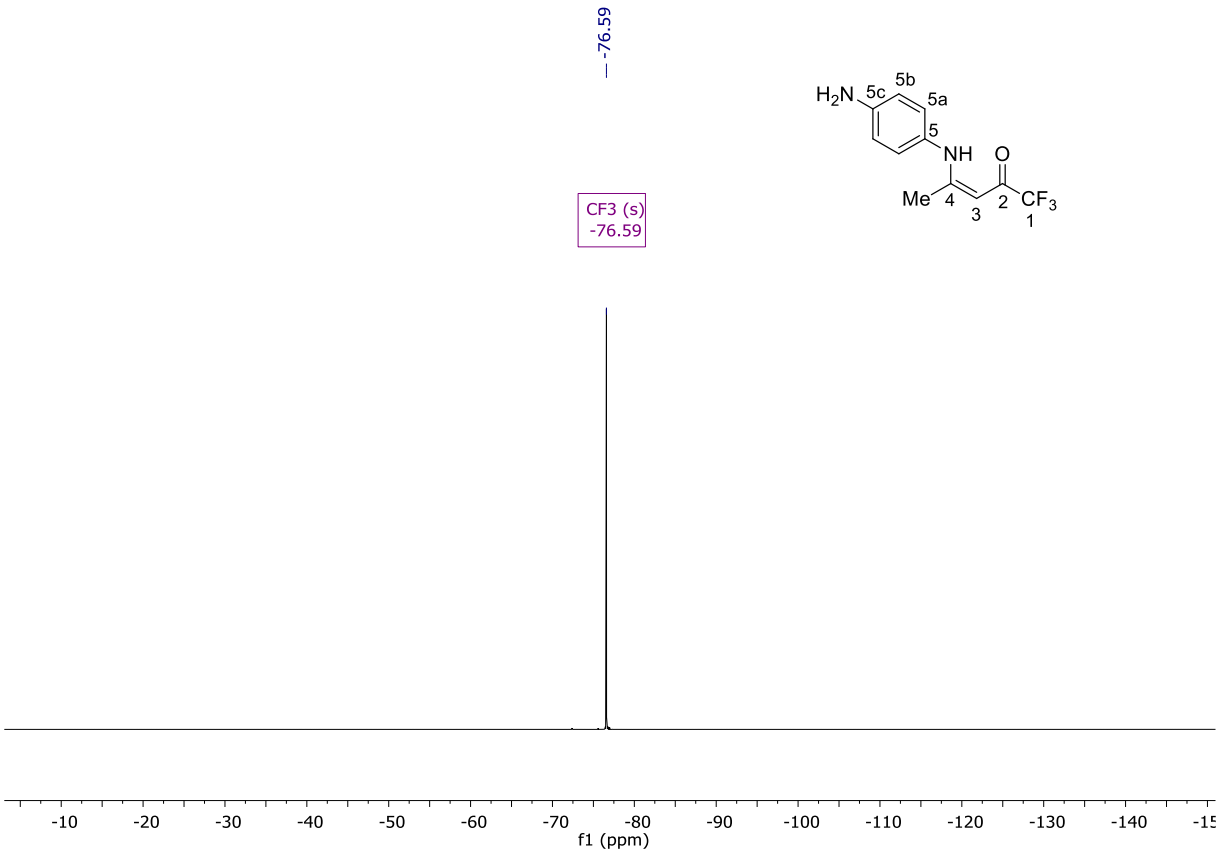

Figure S30. ^{19}F (565 MHz) NMR spectra of **3a** in $CDCl_3$.

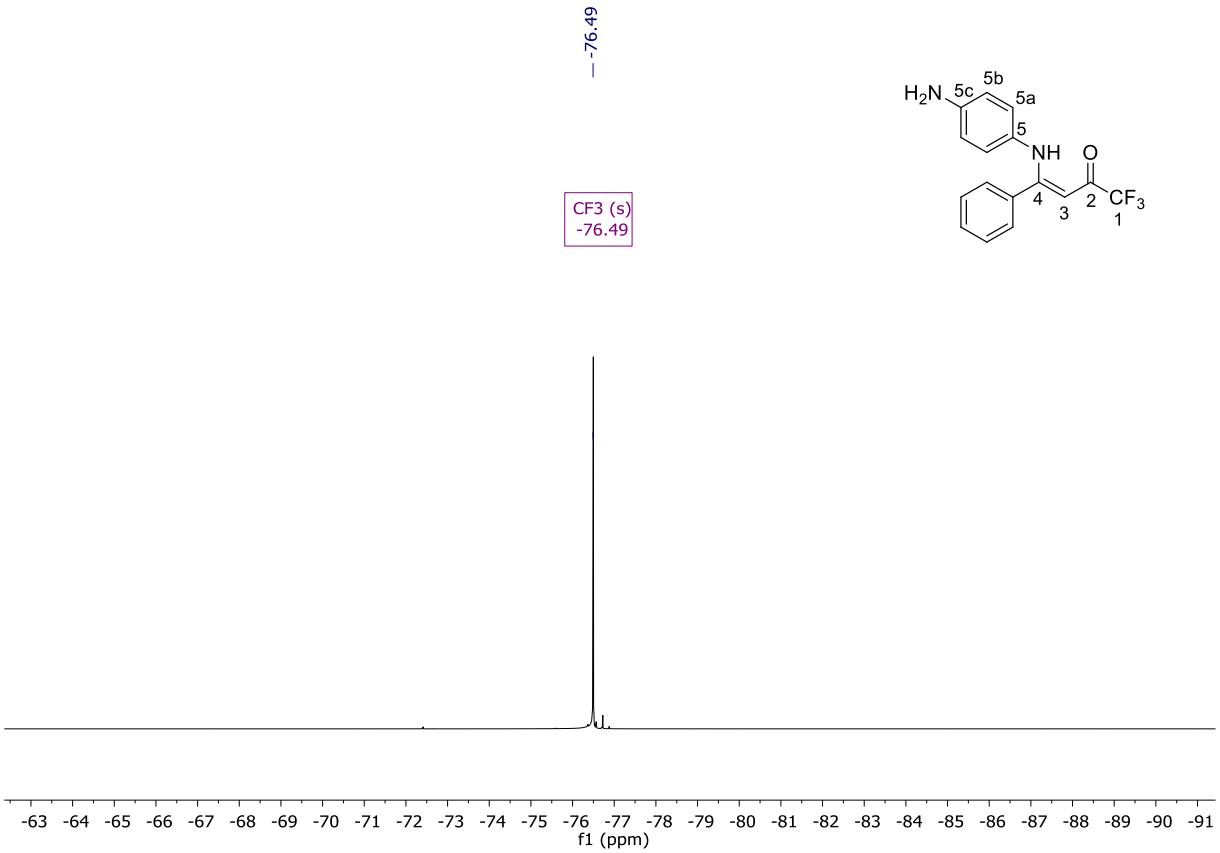

Figure S31. ^{19}F (565 MHz) NMR spectra of **3b** in $CDCl_3$.

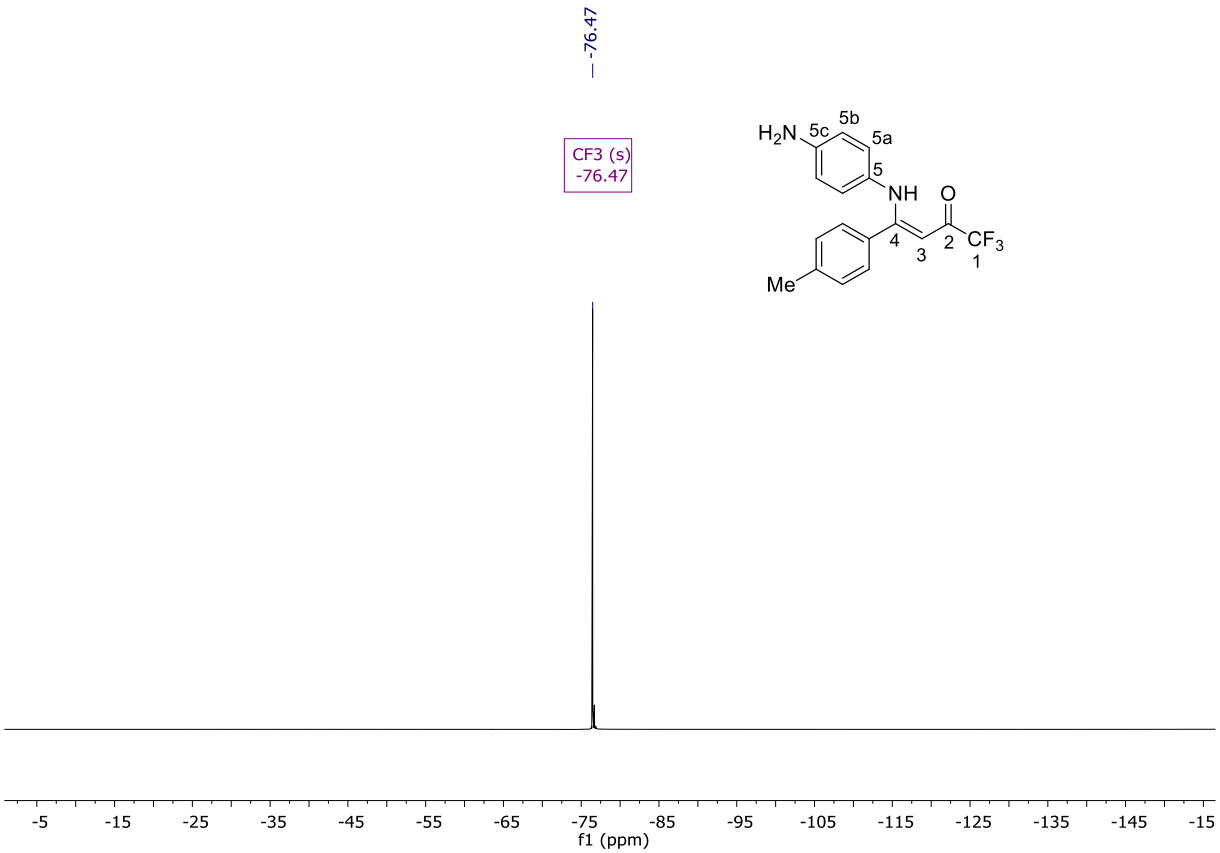

Figure S32. ^{19}F (565 MHz) NMR spectra of **3c** in $CDCl_3$.

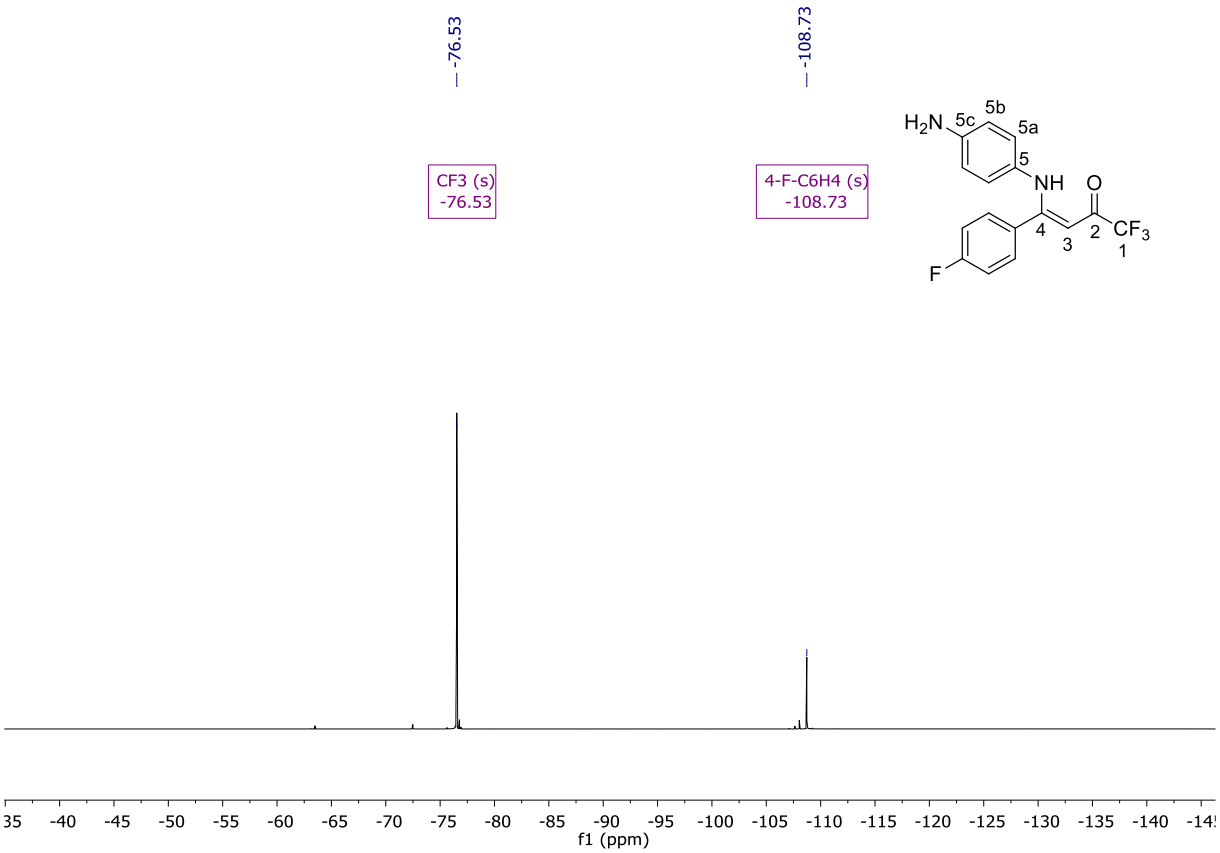

Figure S33. ^{19}F (565 MHz) NMR spectra of **3d** in $CDCl_3$.

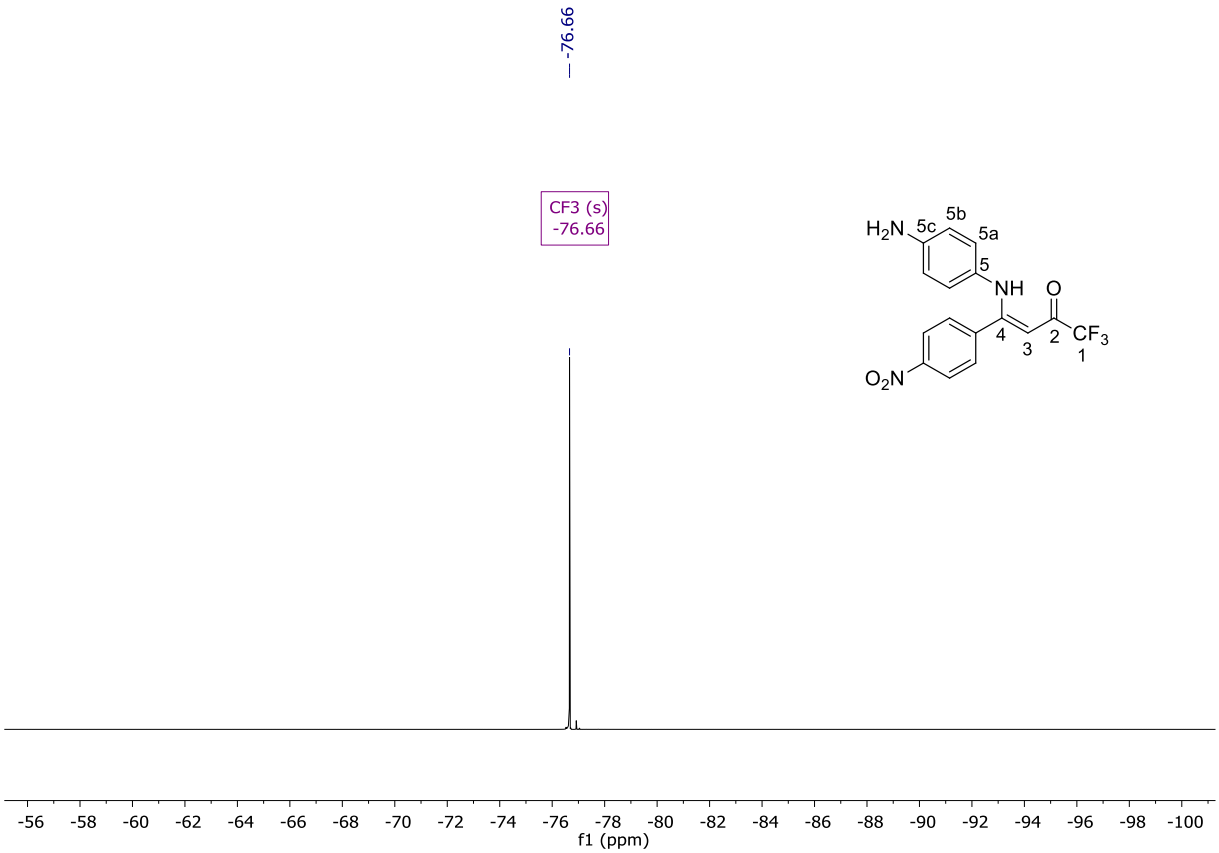

Figure S34. ^{19}F (565 MHz) NMR spectra of **3e** in $CDCl_3$.

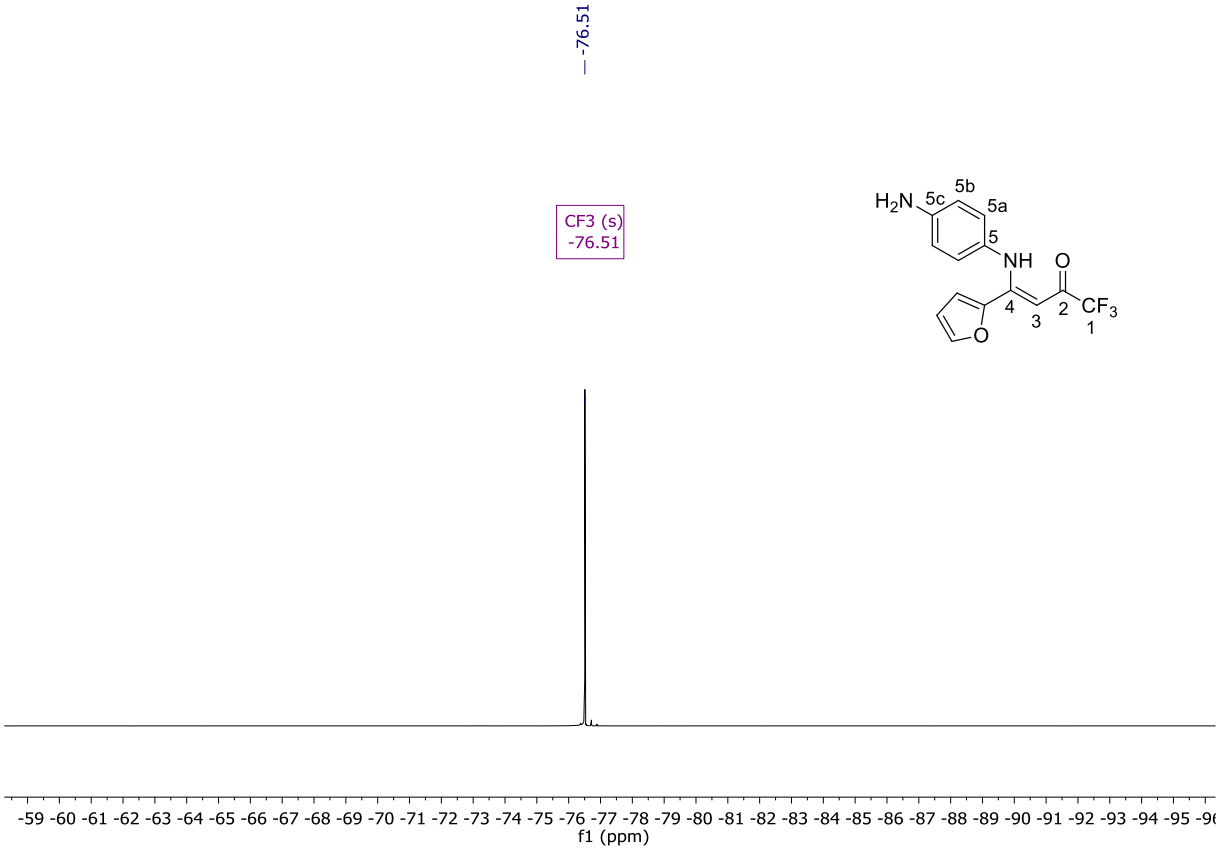

Figure S35. ^{19}F (565 MHz) NMR spectra of **3f** in $CDCl_3$.

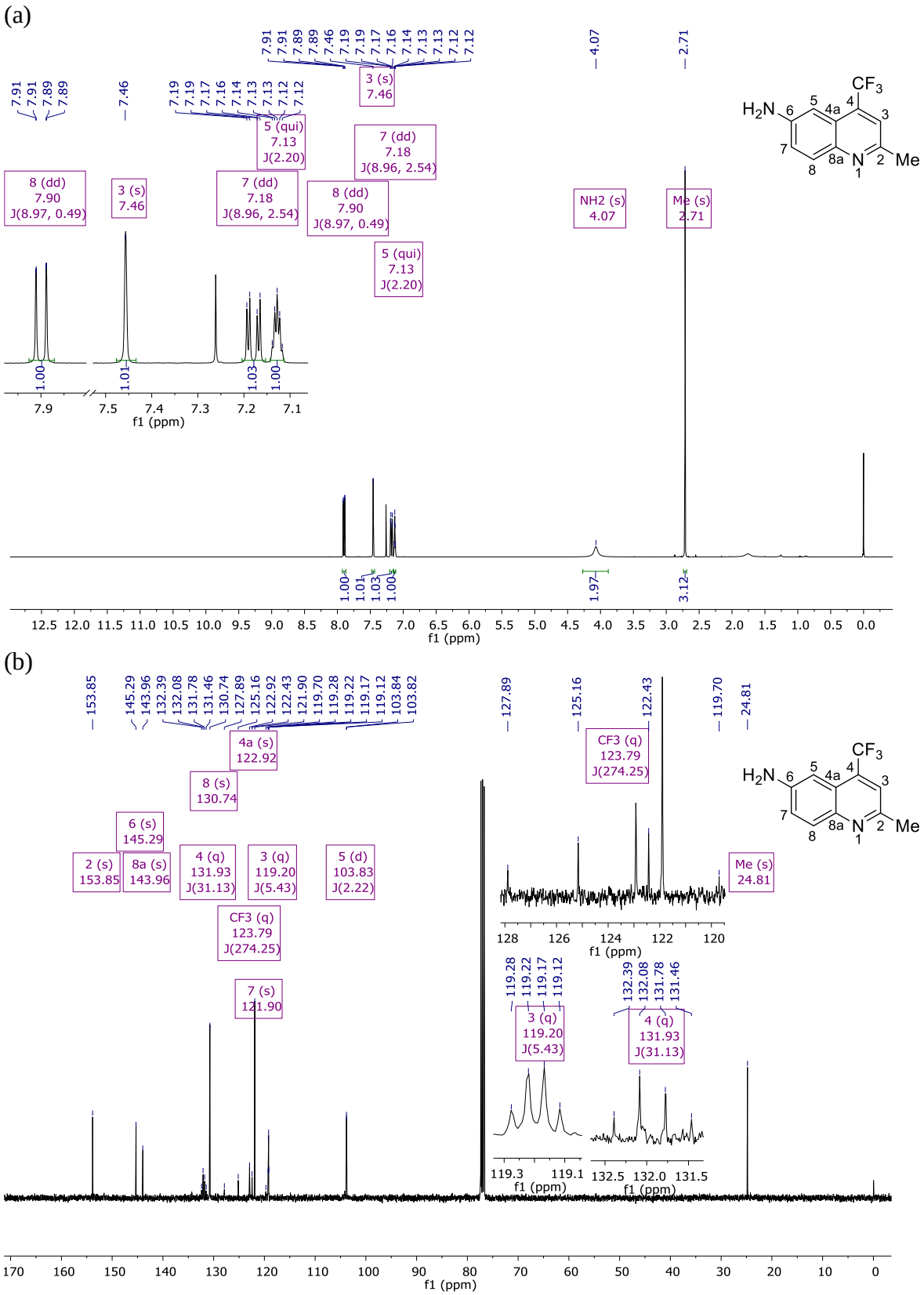

Figure S36. (a) ^{1}H (400 MHz) and (b) ^{13}C (100 MHz) NMR spectra of **4a** in $CDCl_3$.

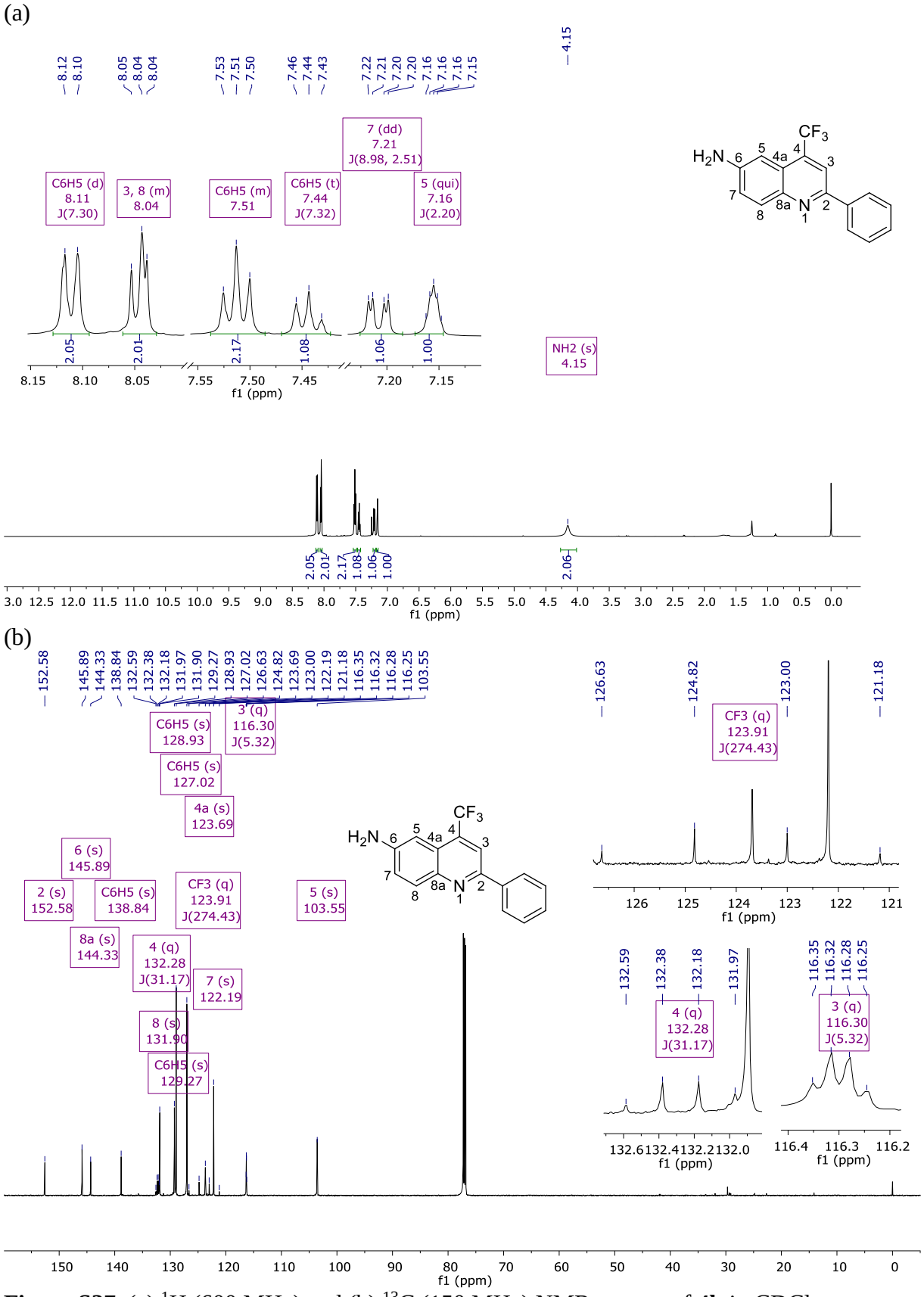

Figure S37. (a) ^{1}H (600 MHz) and (b) ^{13}C (150 MHz) NMR spectra of **4b** in $CDCl_3$.

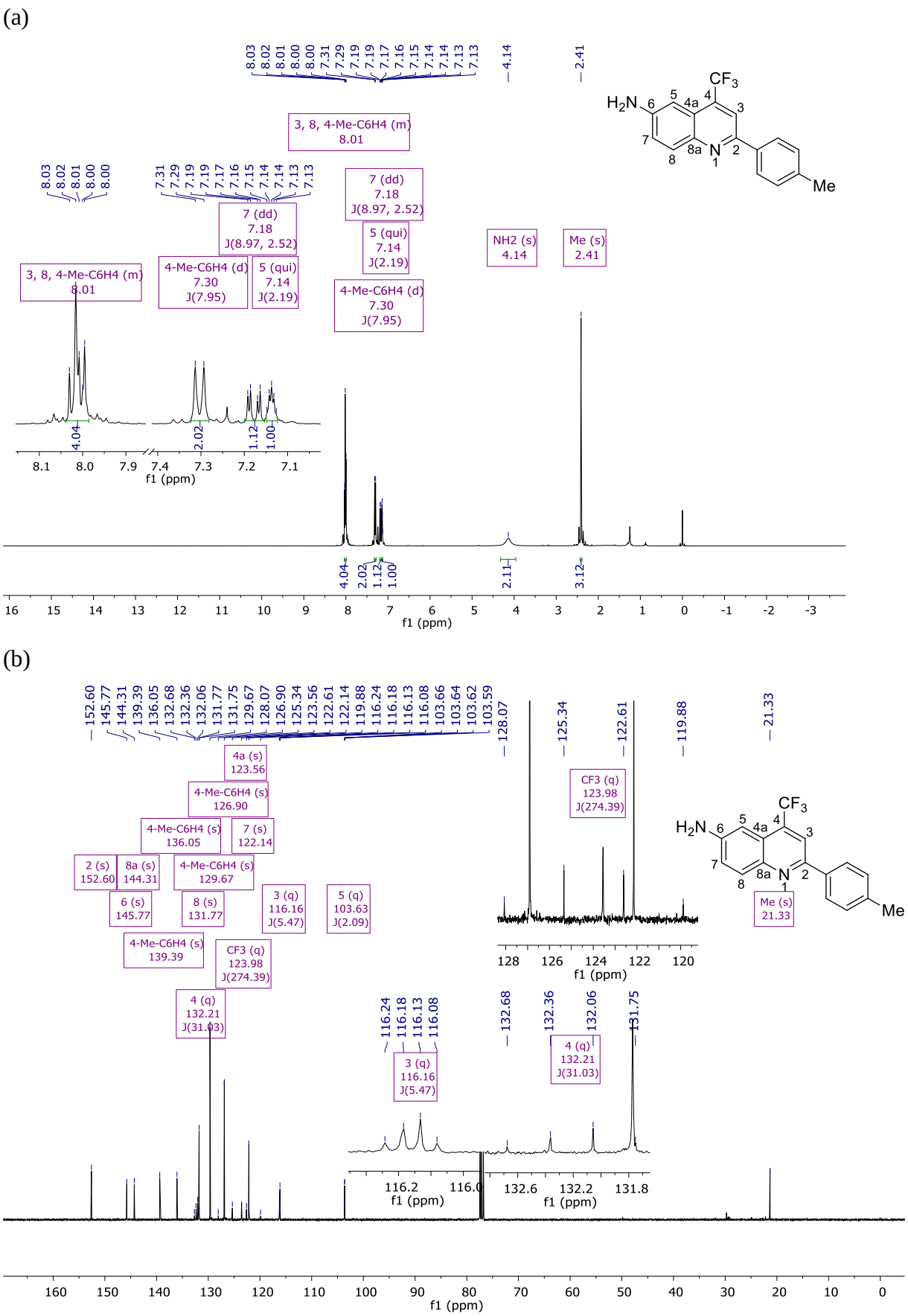

Figure S38. (a) ^{1}H (400 MHz) and (b) ^{13}C (100 MHz) NMR spectra of **4c** in $CDCl_3$.

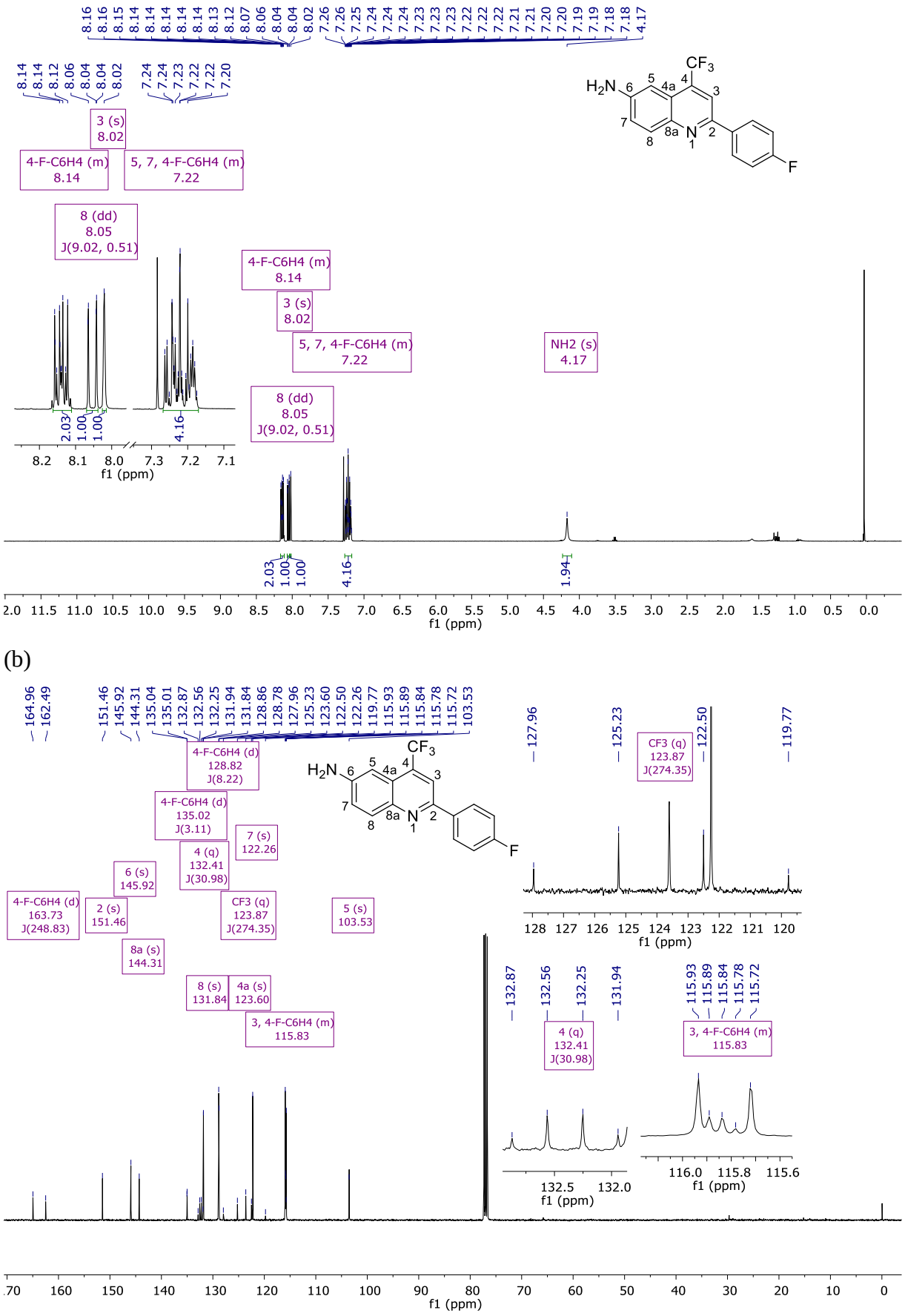

Figure S39. (a) ^{1}H (400 MHz) and (b) ^{13}C (100 MHz) NMR spectra of **4d** in $CDCl_3$.

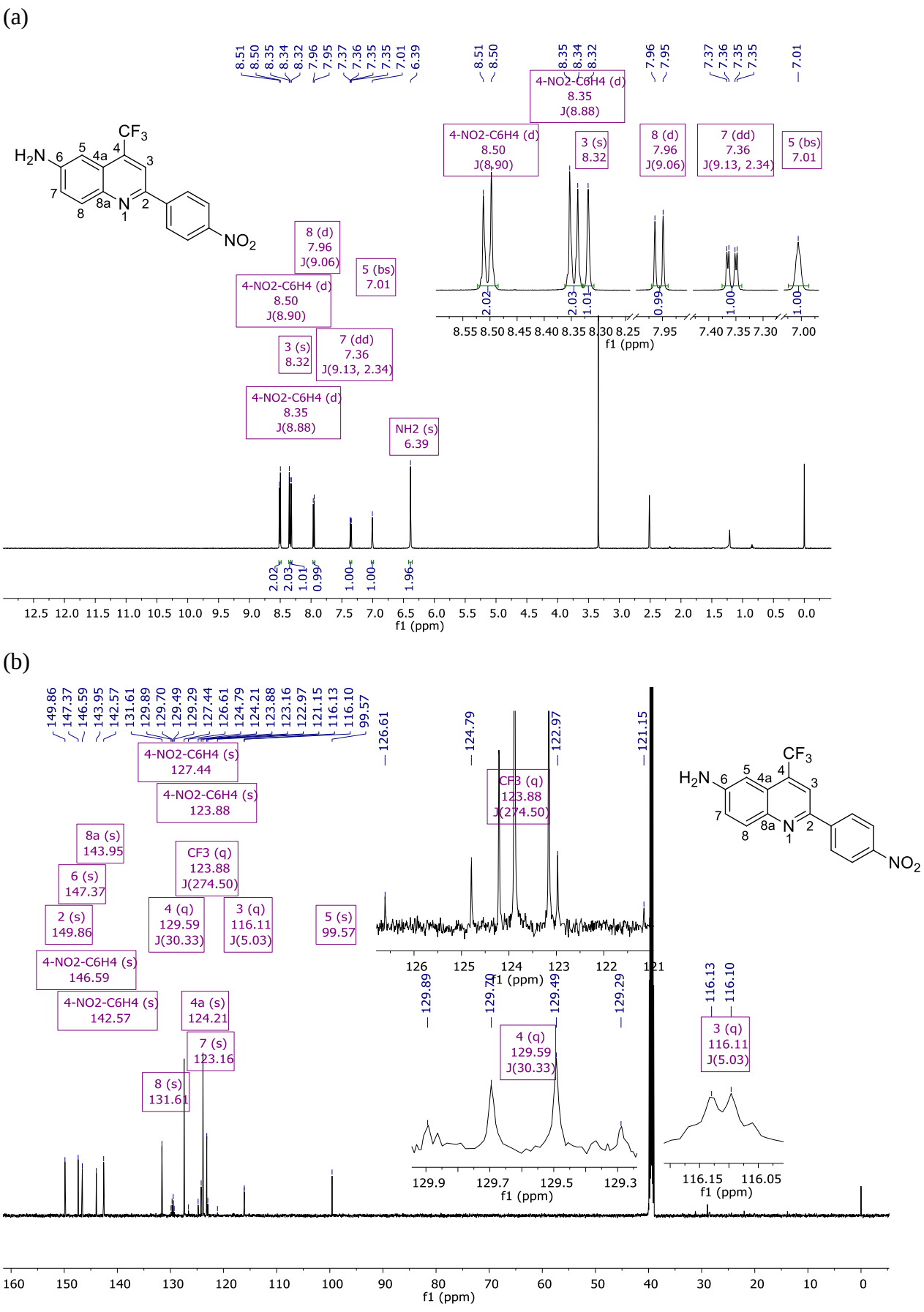

Figure S40. (a) ^{1}H (600 MHz) and (b) ^{13}C (150 MHz) NMR spectra of **4e** in DMSO-d_6.

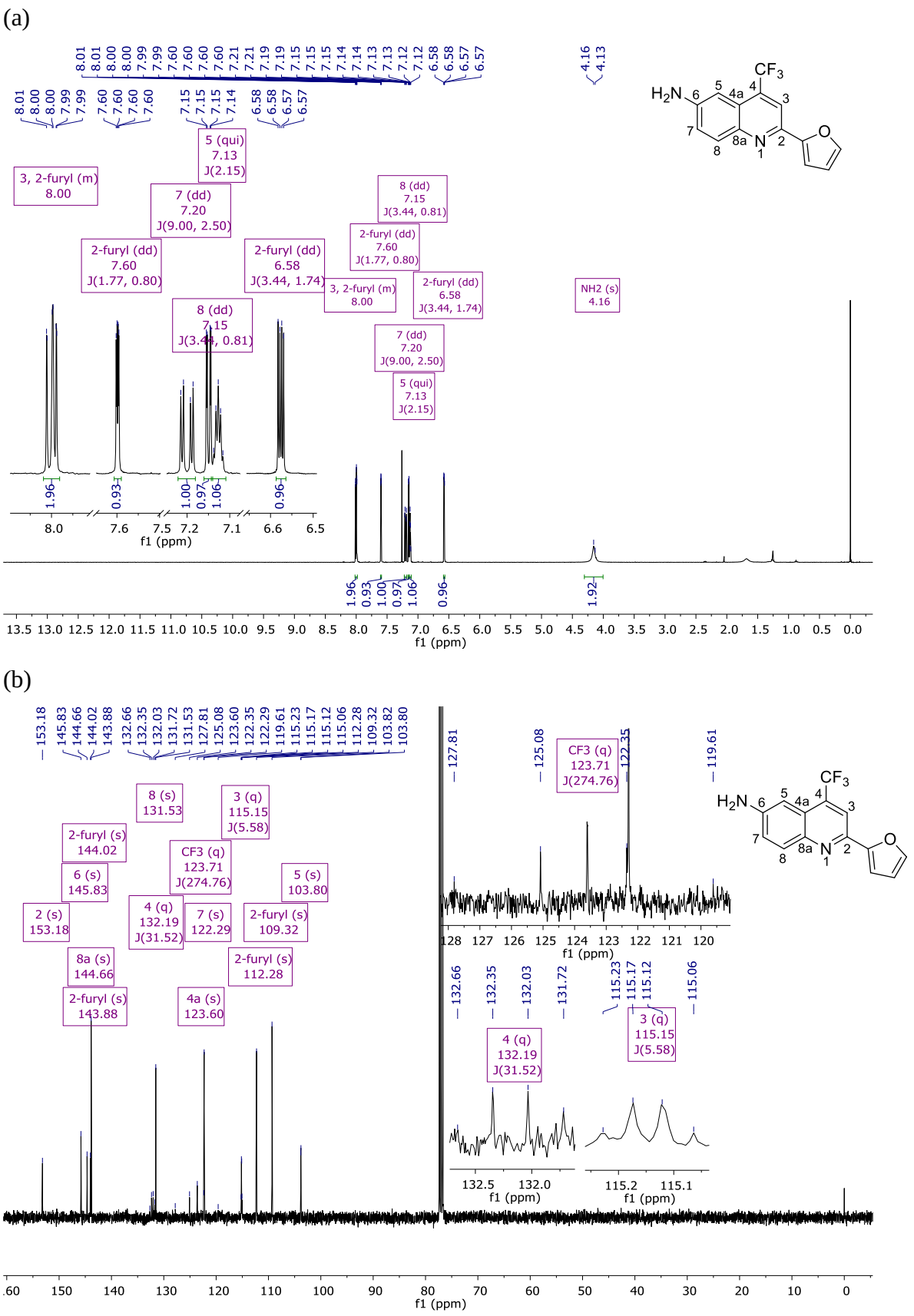

Figure S41. (a) ^{1}H (400 MHz) and (b) ^{13}C (100 MHz) NMR spectra of **4f** in $CDCl_3$.

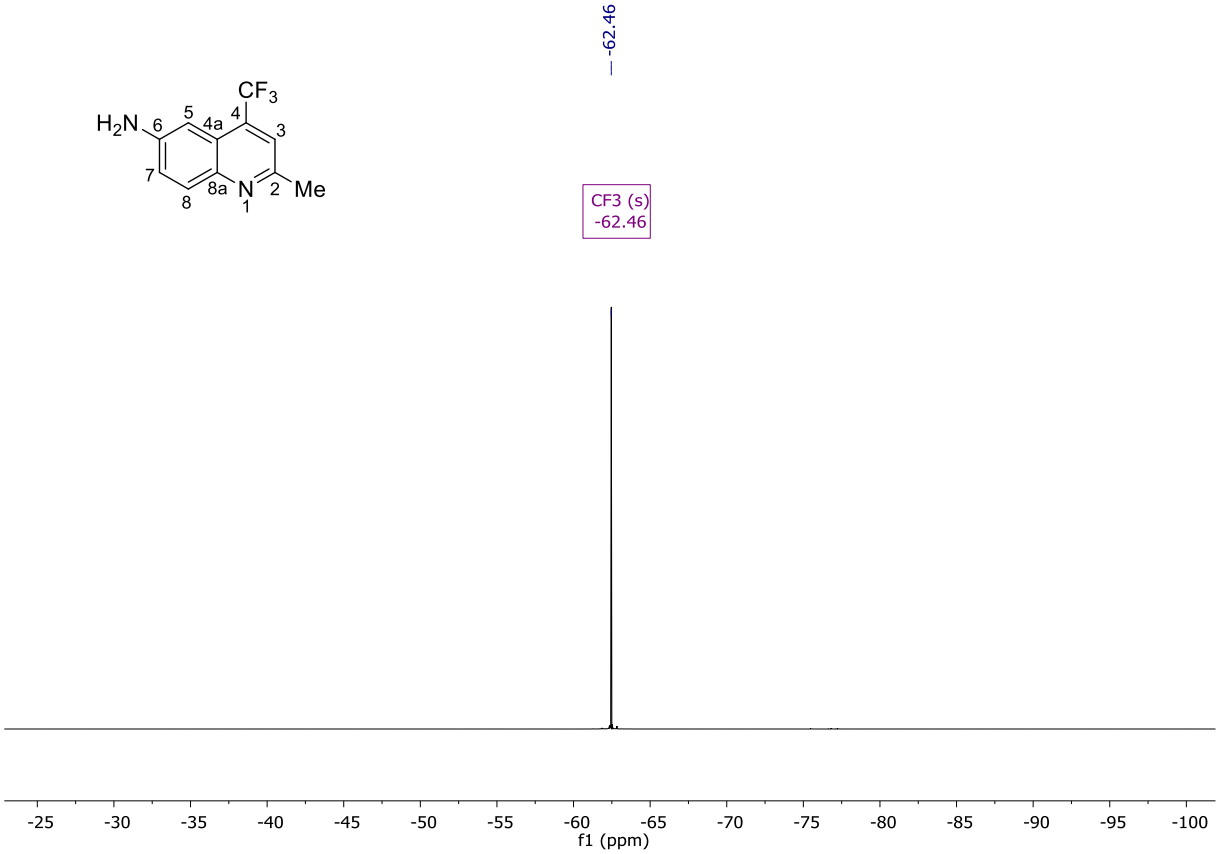

Figure S42. ^{19}F (565 MHz) NMR spectra of **4a** in $CDCl_3$

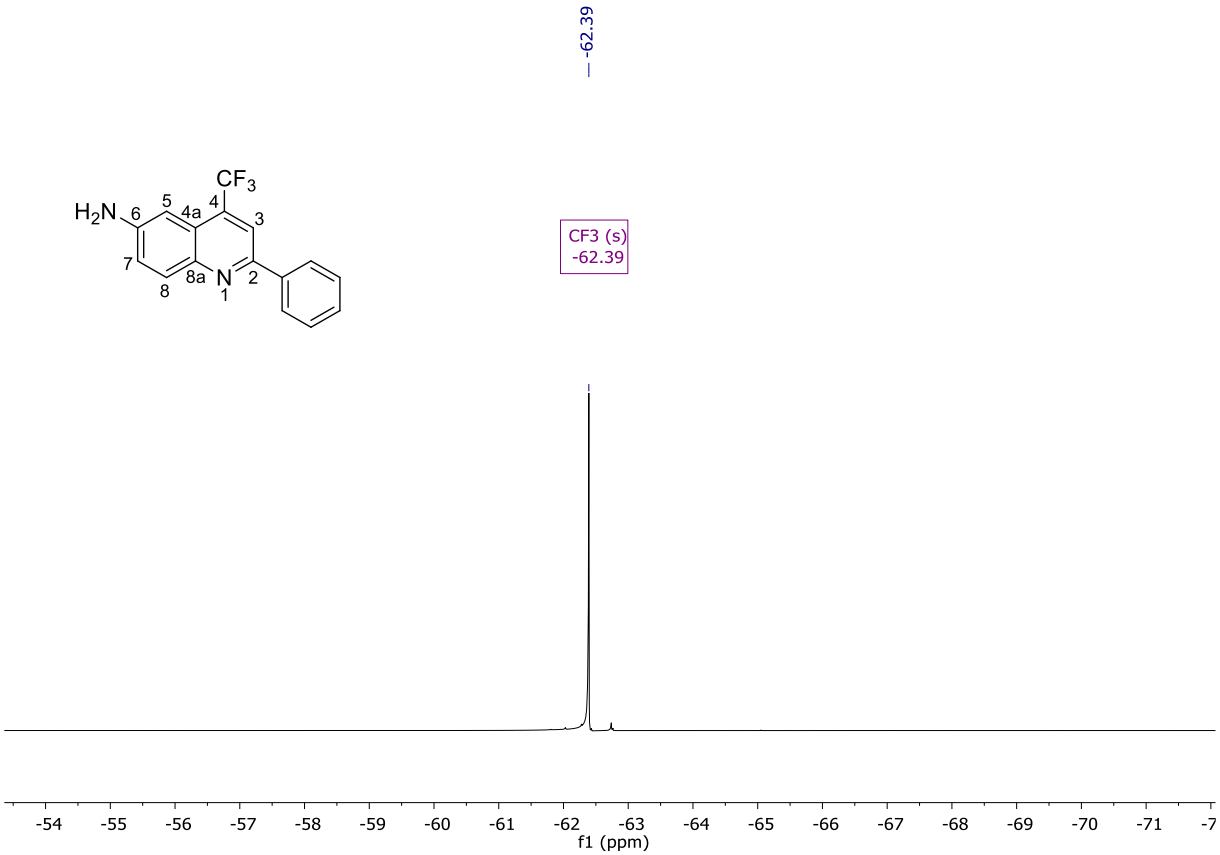

Figure S43. ^{19}F (565 MHz) NMR spectra of **4b** in $CDCl_3$.

Figure S44. ^{19}F (565 MHz) NMR spectra of **4c** in $CDCl_3$.

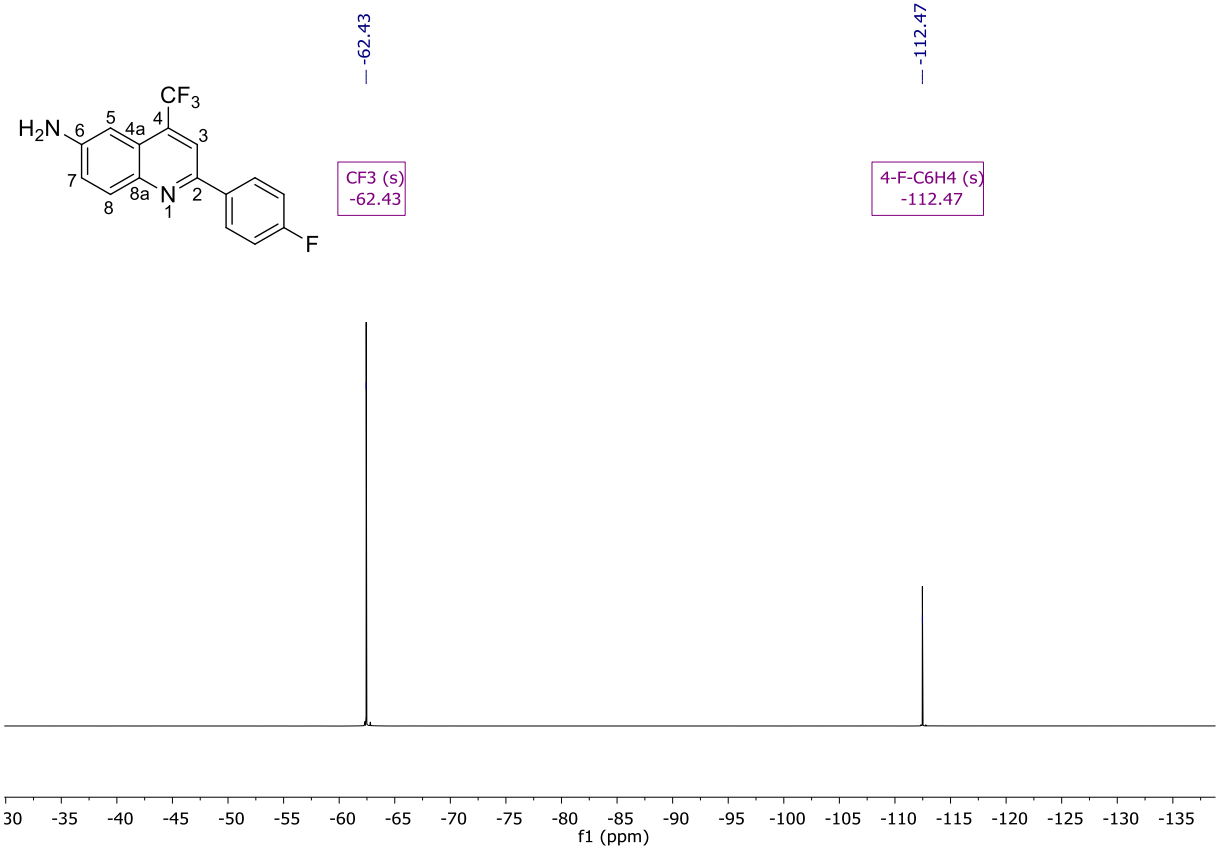

Figure S45. ^{19}F (565 MHz) NMR spectra of **4d** in $CDCl_3$.

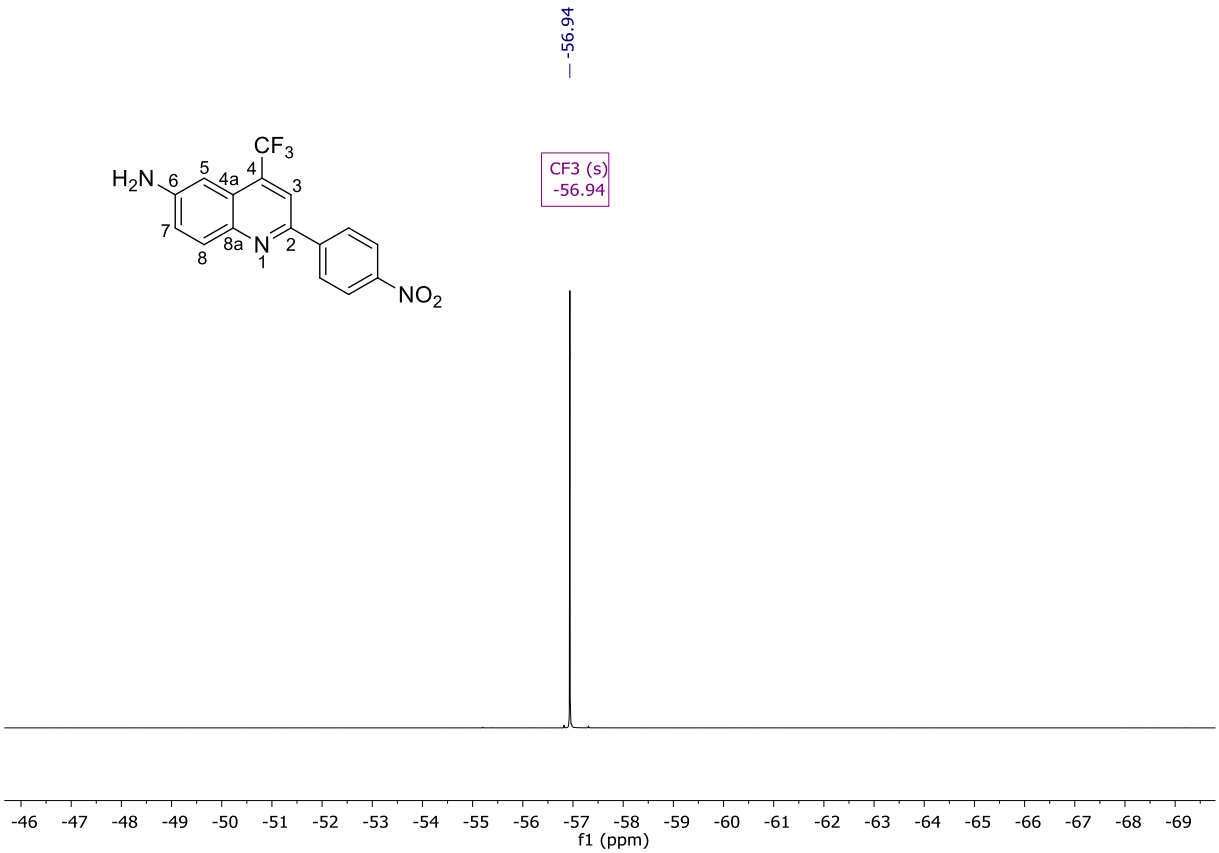

Figure S46. ^{19}F (565 MHz) NMR spectra of **4e** in DMSO-d_6.

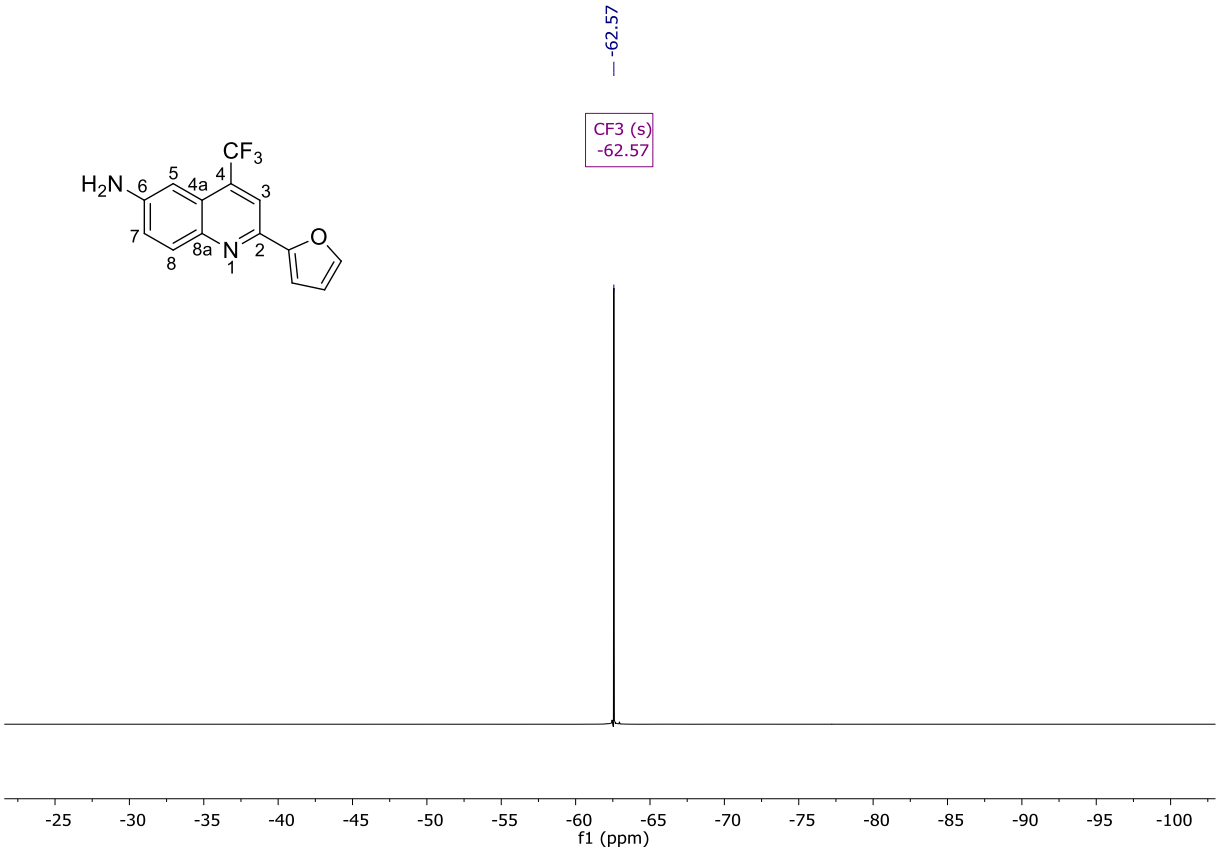

Figure S47. ^{19}F (565 MHz) NMR spectra of **4f** in $CDCl_3$.

8. HRMS Spectra

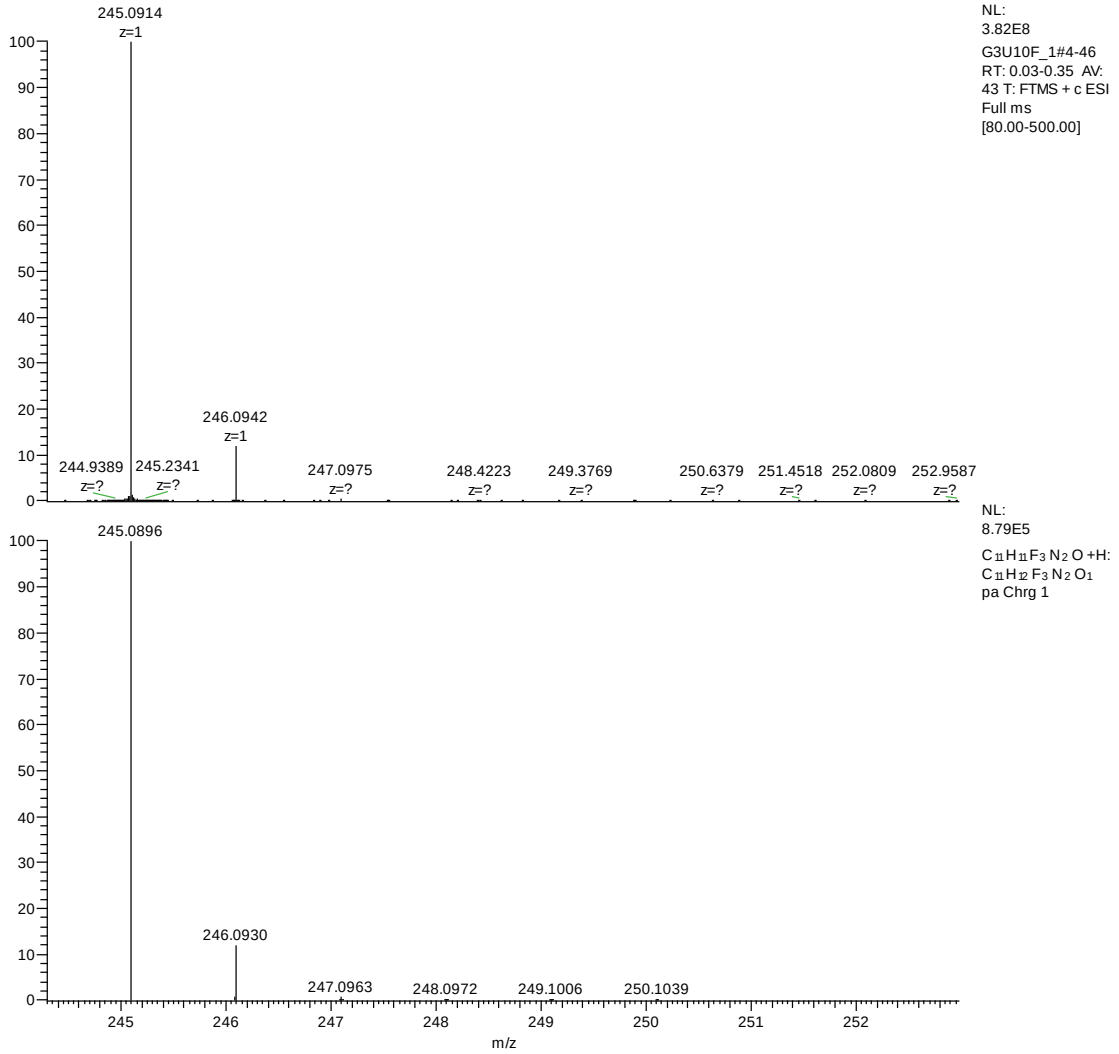

Figure S48. HRMS spectrum of **3b** (experimental up, calculated down).

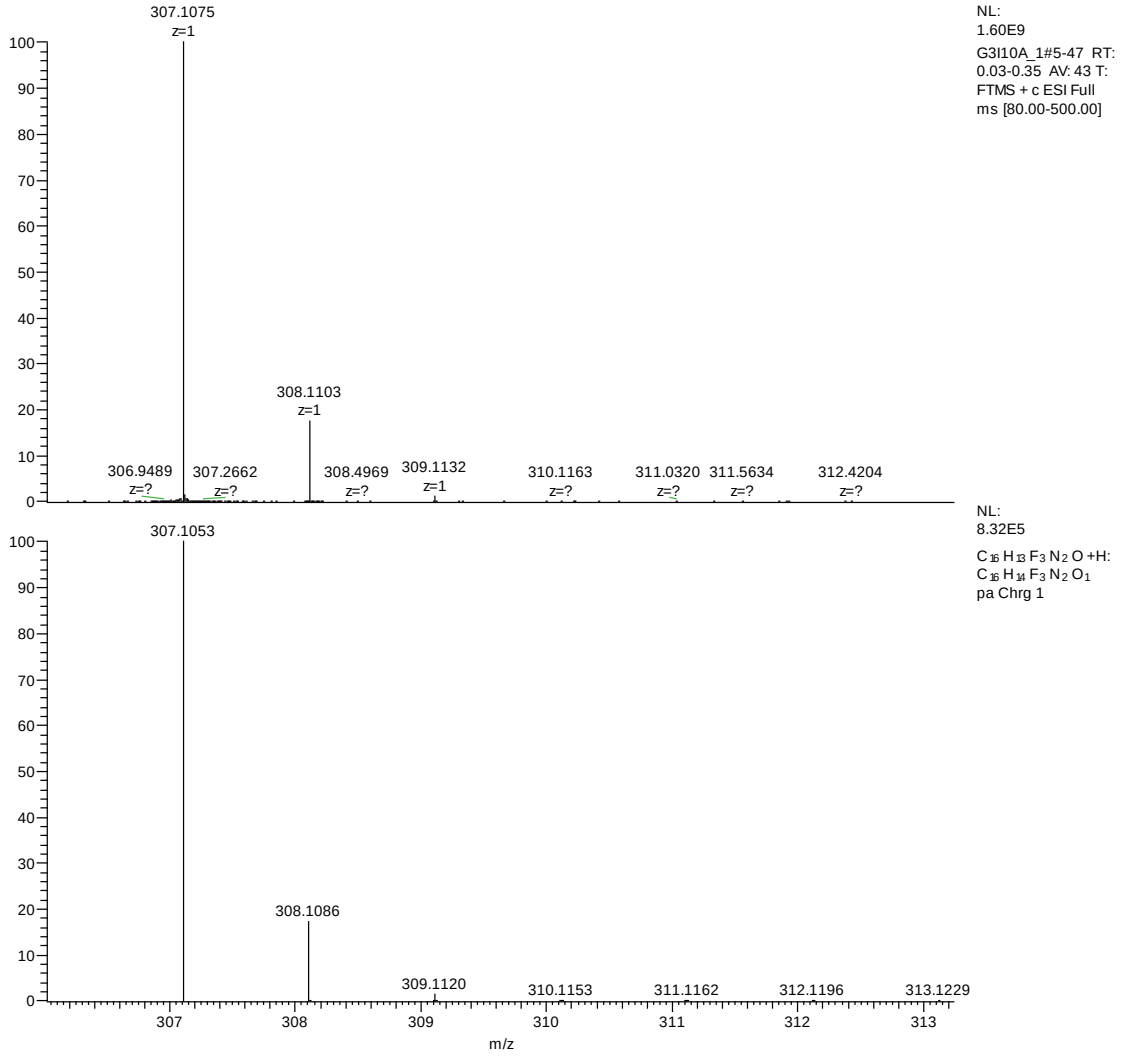

Figure S49. HRMS spectrum of **3b** (experimental up, calculated down).

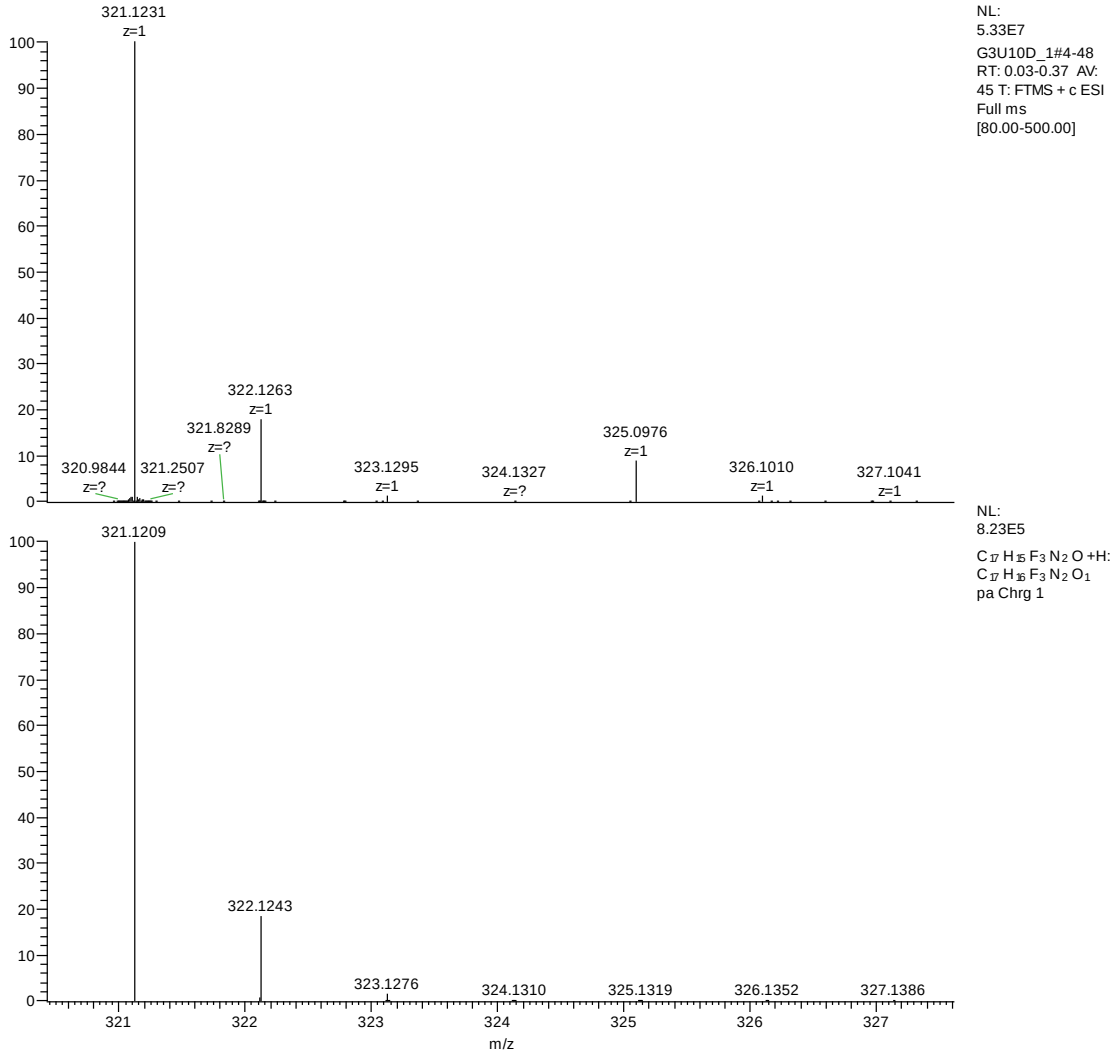

Figure S50. HRMS spectrum of **3c** (experimental up, calculated down).

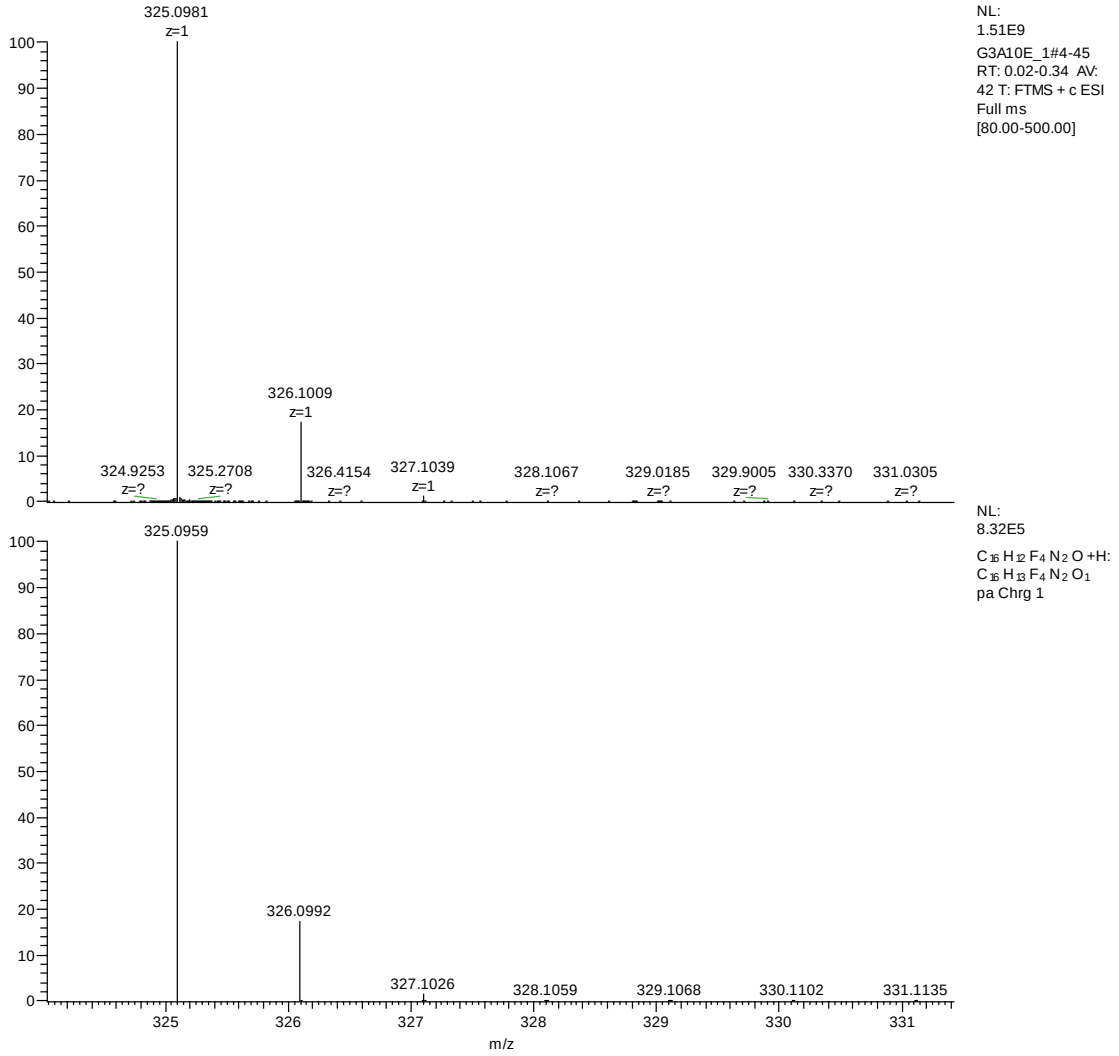

Figure S51. HRMS spectrum of **3d** (experimental up, calculated down).

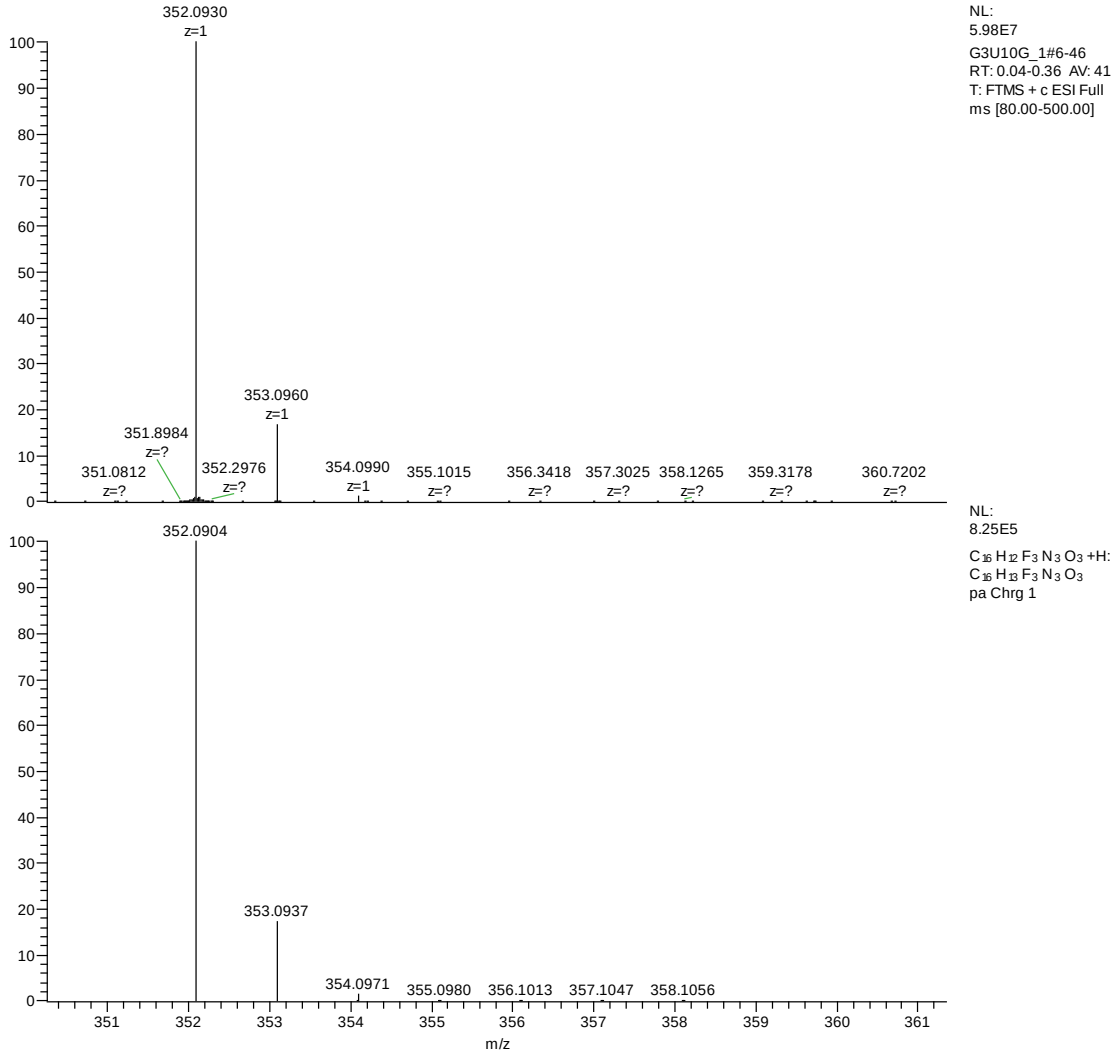

Figure S52. HRMS spectrum of **3e** (experimental up, calculated down).

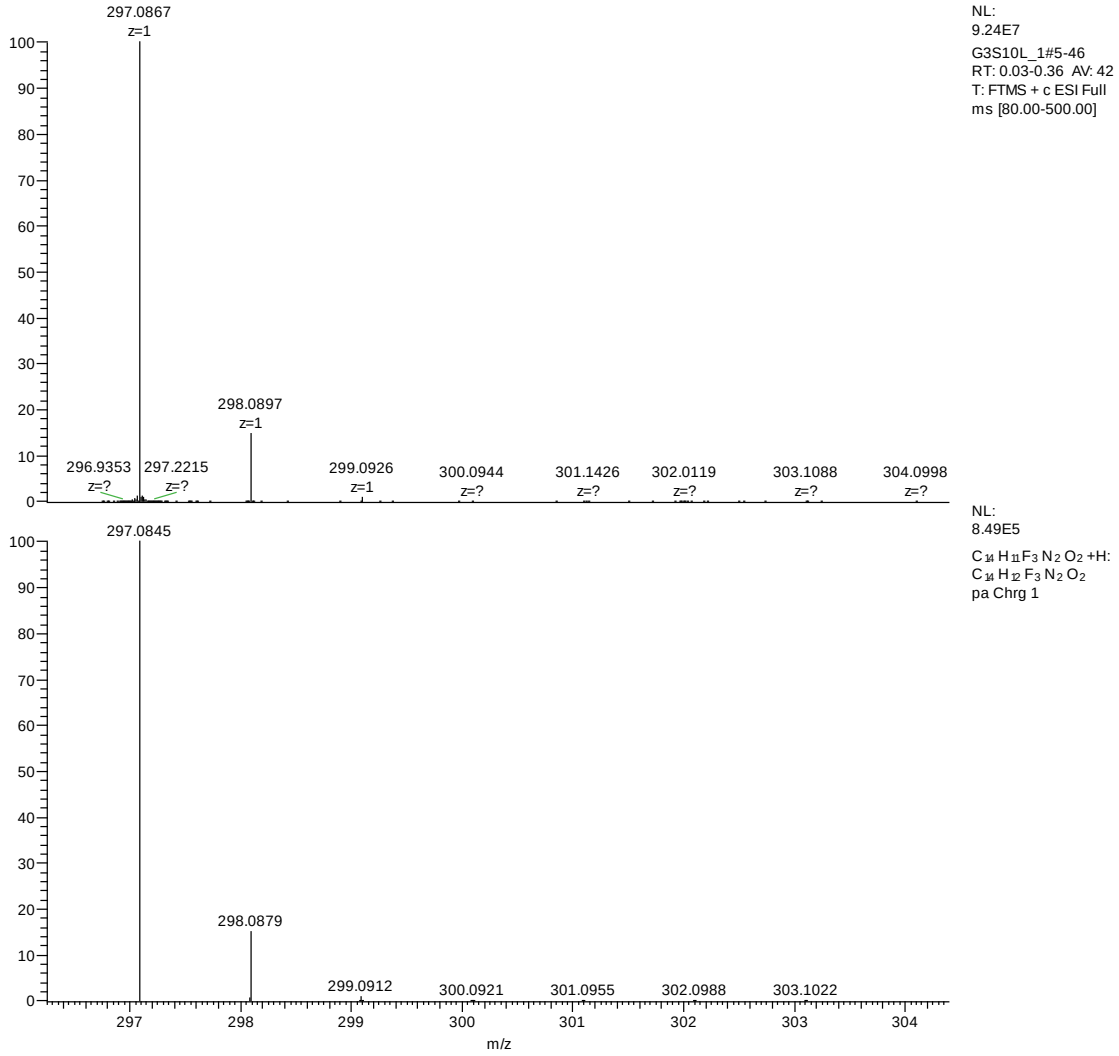

Figure S53. HRMS spectrum of **3f** (experimental up, calculated down).

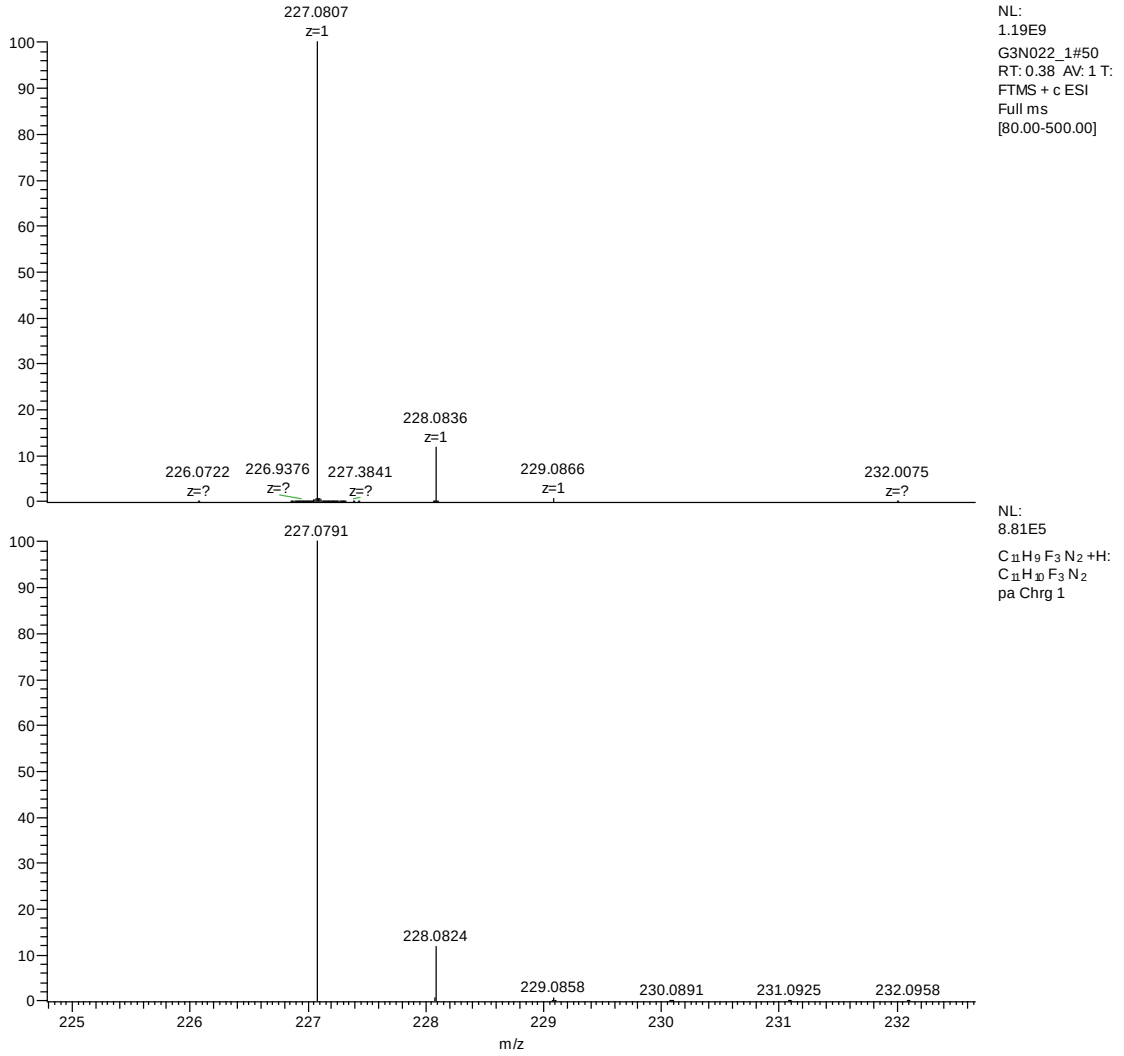

Figure S54. HRMS spectrum of **4a** (experimental up, calculated down).

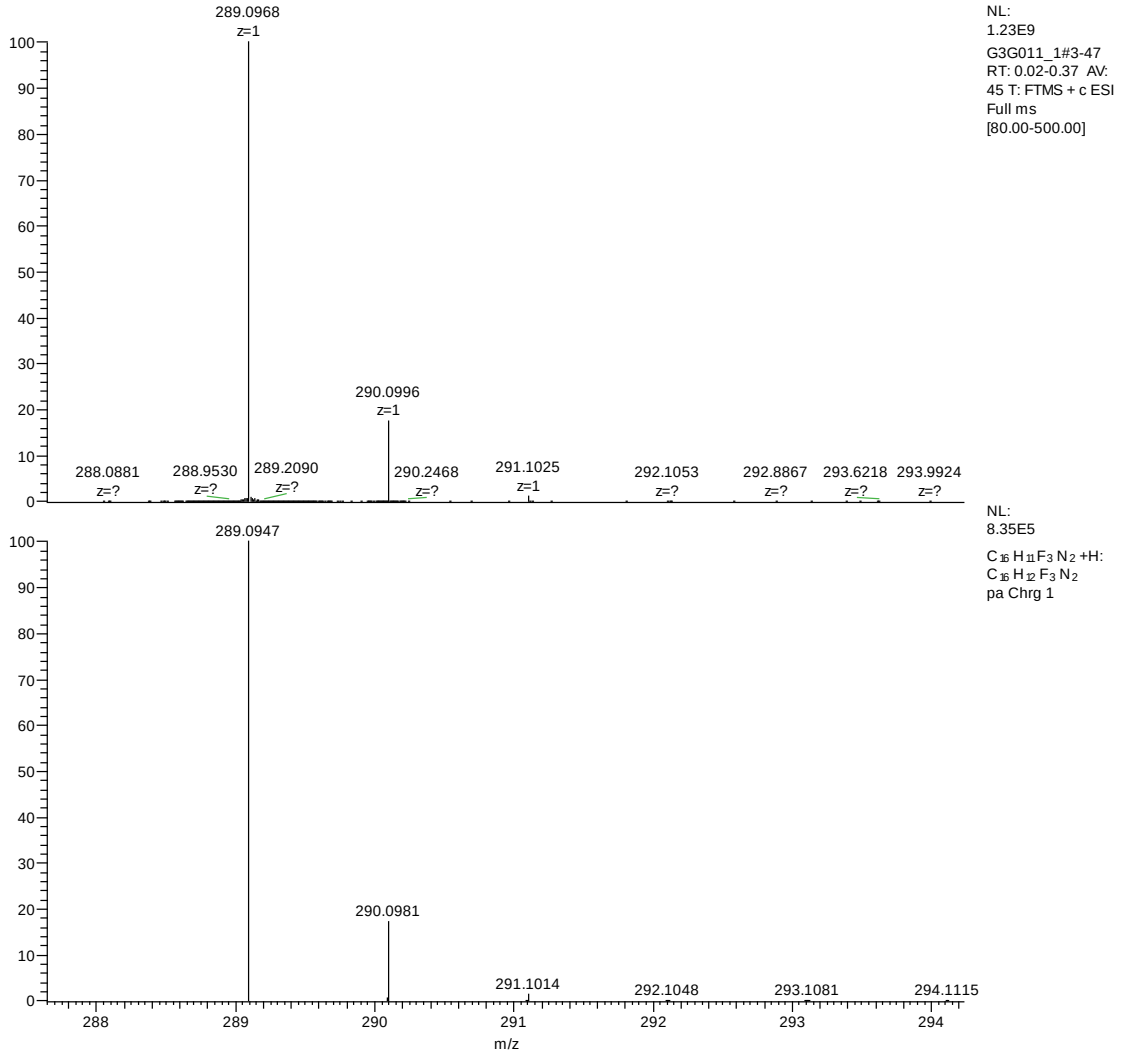

Figure S55. HRMS spectrum of **4b** (experimental up, calculated down).

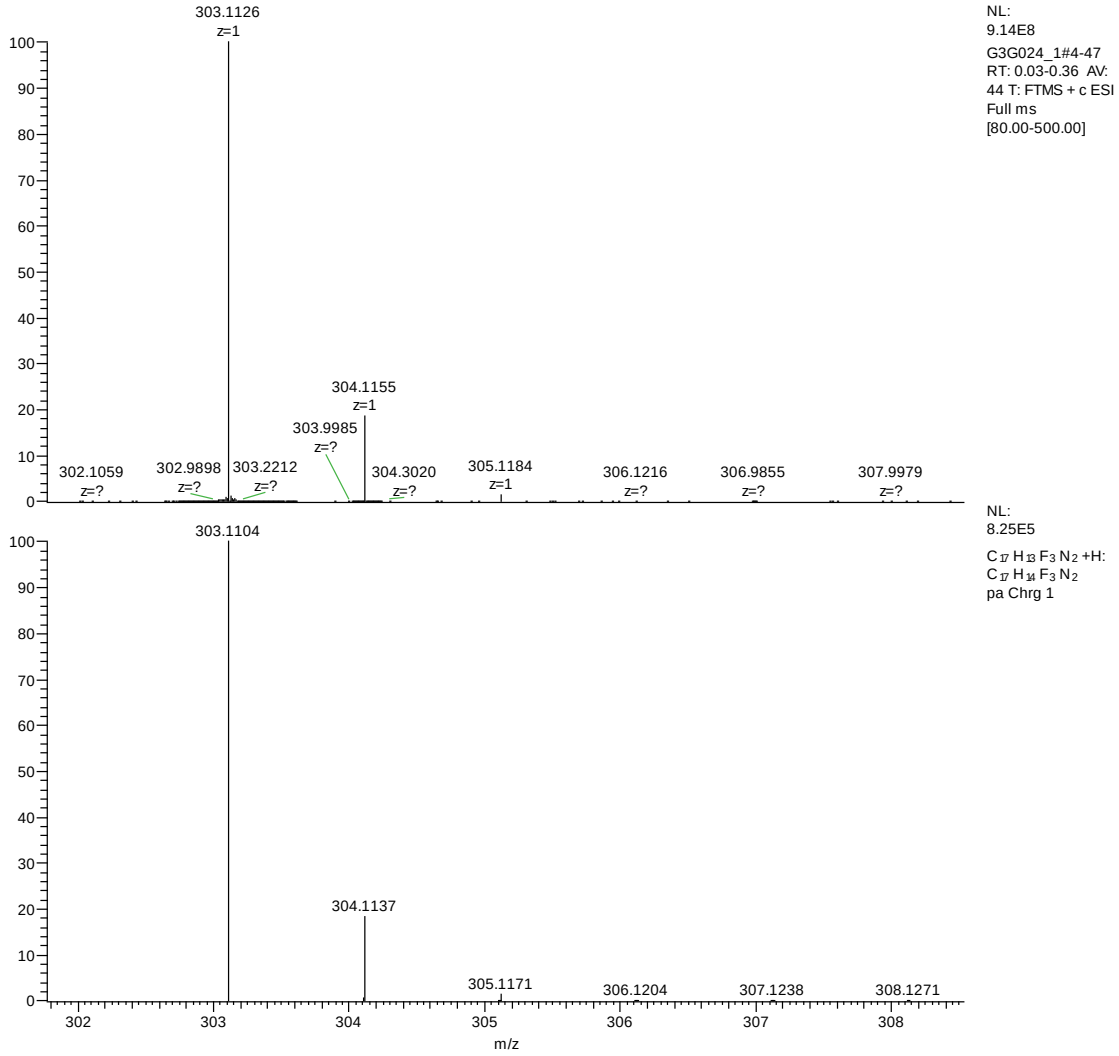

Figure S56. HRMS spectrum of **4c** (experimental up, calculated down).

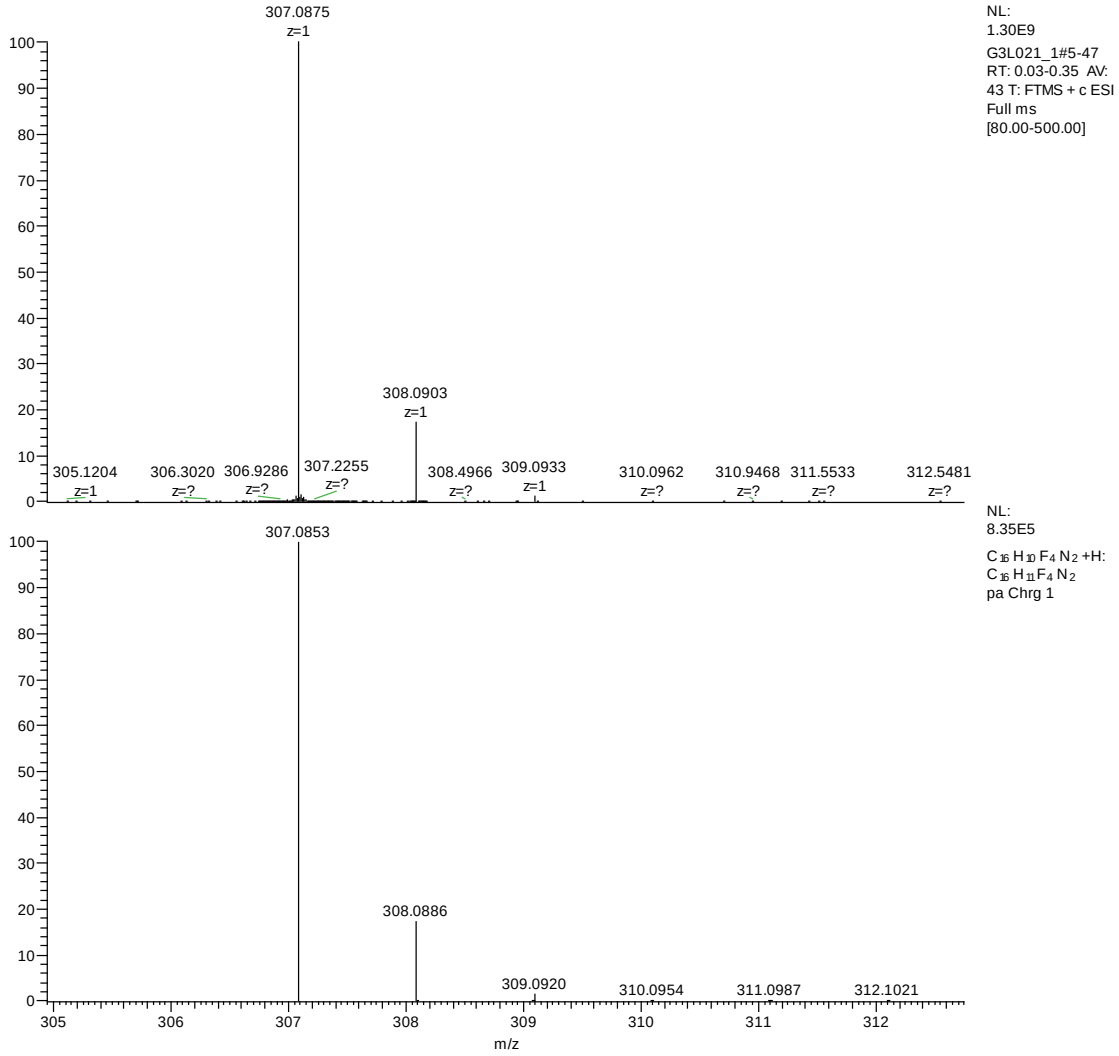

Figure S57. HRMS spectrum of **4d** (experimental up, calculated down).

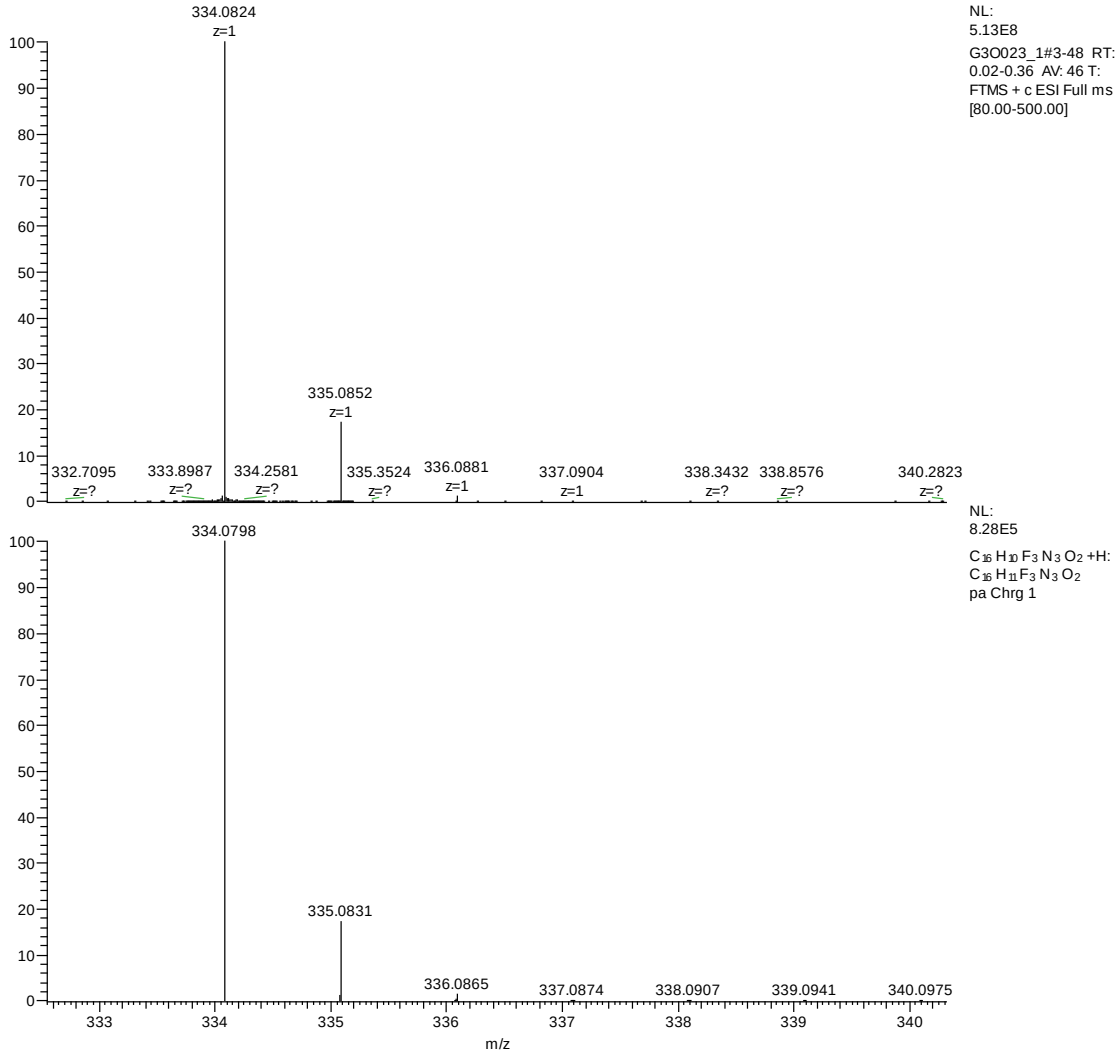

Figure S58. HRMS spectrum of **4e** (experimental up, calculated down).

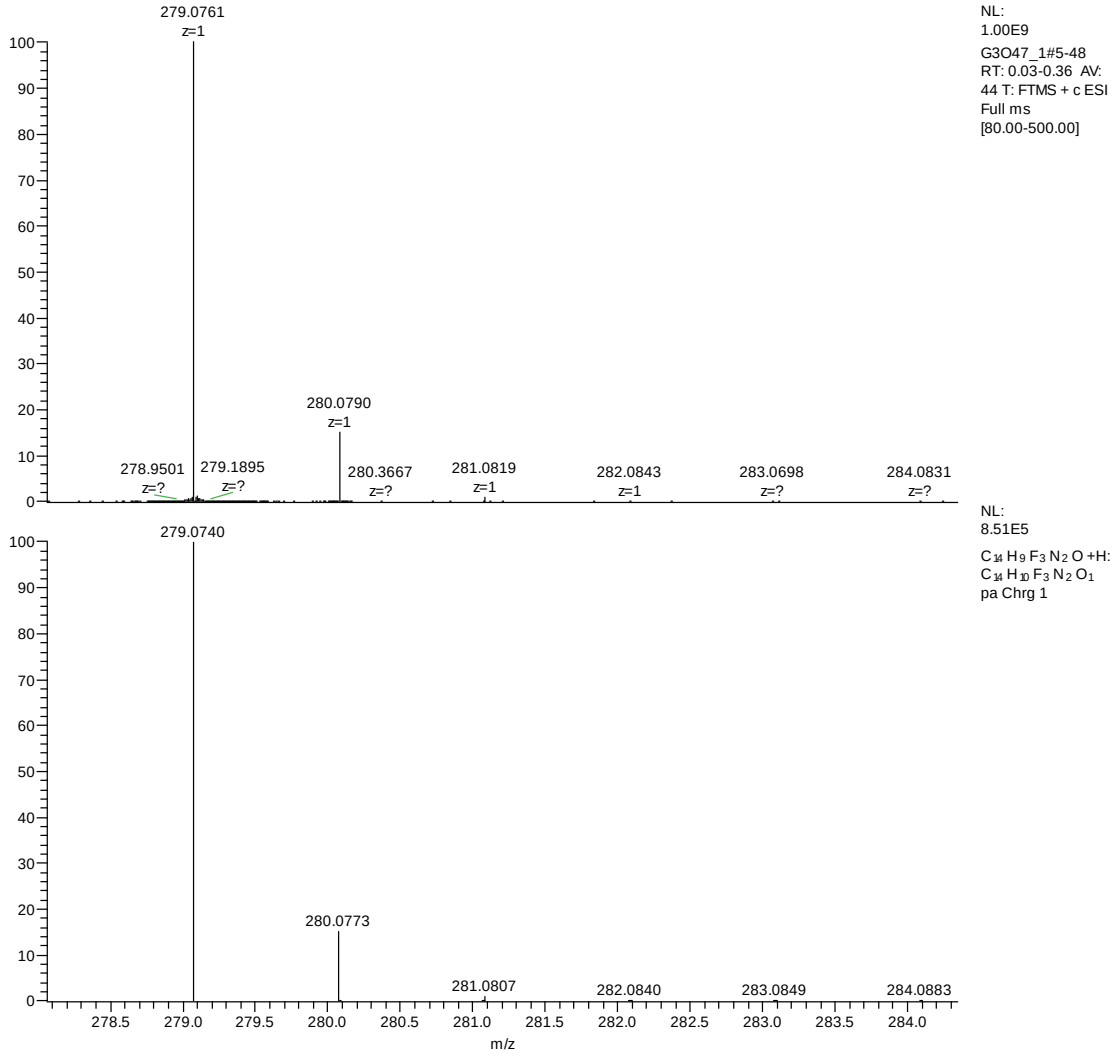

Figure S59. HRMS spectrum of **4f** (experimental up, calculated down).